Manuel Naveiro
Manuel Romero Gómez
Ignacio Arias-Fernández
Álvaro Baaliña Insua

http://dx.doi.org/10.21278/brod74203

ISSN 0007-215X
eISSN 1845-5859

Energy, exergy, economic and environmental analysis of a regasification system integrating simple ORC and LNG open power cycle in floating storage regasification units

UDC 665.72:621.48
Original scientific paper

Summary

A thermodynamic, economic and environmental analysis of a regasification system including a simple Organic Rankine Cycle (ORC) and an Open Organic Rankine Cycle (OC) to utilise the liquefied natural gas (LNG) cold energy is carried out in the present paper. The proposed system, called ORC-OC, uses ambient seawater as heat source (open loop) and is implemented on board a Floating Storage Regasification Unit (FSRU) in order to reduce the greenhouse gas (GHG) emissions associated with the electricity generation plant, i.e., dual fuel (DF) engines. Regarding the ORC working fluids analysed, an ethane/propane zeotropic mixture is applied. The ORC-OC is compared with the simple ORC architecture, giving the first one better energy (lower specific energy consumption), exergy (higher exergy efficiency) and environmental (lower CO_2e emissions) results. When compared to the regasification systems installed on board, the ORC-OC system reduces the specific energy consumption by 86.99 % and increases the exergy efficiency by 17.82 % with respect to the most efficient conventional system installed on FSRUs (direct seawater regasification system), leading to a reduction of CO_2e emissions of more than 80 %. In addition, the ORC-OC system is more cost-effective than conventional regasification systems when the LNG price is above 6,508 USD/MMBtu.

Key words: *Floating Storage Regasification Unit; zeotropic mixture; exergy analysis; liquefied natural gas cold energy; organic Rankine*

NOMENCLATURE

Abbreviations

AC/NGH	after cooler/natural gas heater
BOG	boil off gas
BOR	boil off rate
CD	condenser
CEPCI	Chemical Engineering Plant Cost Index
CFRI	Carbon Footprint Regasification Indicator
CP	centrifugal pump
DF	dual fuel
DFDE	dual fuel diesel electric
DO	diesel oil
EERI	Energy Efficiency Regasification Indicator
FCI	fixed capital investment
FSRU	floating storage regasification unit
FV	forcing vaporizer
GCU	gas combustion unit
GCU-OL	seawater regasification system without recondenser
GHG	greenhouse gas
GWP	global warming potential
LD	low duty
LNG	liquefied natural gas
MX	mixer
NG	natural gas
OC	open organic Rankine cycle
ORC	organic Rankine cycle
ORC-CC-CL	closed loop regasification system with ORC and carbon capture
ORC-OC	closed organic Rankine cycle with open organic Rankine cycle
2ORC-OC	two-stage closed organic Rankine cycle with open organic Rankine cycle
3ORC-OC	three-stage closed organic Rankine cycle with open organic Rankine cycle
ORC-OL	open loop propane regasification system with ORC
P	pump
PHE	plate heat exchanger
P-OL	open loop propane regasification system
R	recondenser
S	separator
S&T	shell and tubes heat exchanger
SW-OL	seawater regasification system
T	turbine
TH	trim heater
V	valve
VP	vaporizer
WG-CL	closed loop propane regasification system

Symbols

b	specific energy consumption (kJ/kW h)
C_F	carbon factor (-)
$\dot{C}, \dot{Z}$	cost rate (USD/min)
e	specific flow exergy (kJ/kg)
$\dot{E}$	exergy flow rate (kW)
h	specific enthalpy (kJ/kg)
i	annual interest (-)
$\dot{I}$	irreversibilities (kW)
$\dot{m}$	mass flow rate (kg/s)
n	lifetime (years)
p	pressure (bar)
$\dot{Q}$	heat transfer rate (kW)
s	specific entropy (kJ/kg K)
T	temperature (ºC)
v	specific volume (m^3/kg)
$\dot{W}$	power (kW)
β_{CRF}	capital recovery factor (-)

γ_{OM}	operation and maintenance factor (-)
η	efficiency (-)
τ	annual operating hours (h)
φ	chemical exergy factor for fuels (kJ/kg)

Subscripts and Superscripts

0	reference condition
alt	alternator
b	base
ch	chemical
CI	capital investment
comp	compressor
cond	condensables
el	electrical
ex	exergy
f	fuel
i	inlet
LHV	lower heating value
m	mechanical, mixture or mixing
n	natural
o	output
OM	operation and maintenance
p	pressure
ph	physical
SW	seawater
th	thermal
tk	storage tank
tot	total
turb	turbine

1. Introduction

The war between Ukraine and Russia has led to record high prices for natural gas (NG) in Europe in 2022 [1]. Faced with this situation, in order to reduce dependence on NG imported by pipeline from Russia, European countries intend, among other measures, to increase the supply of liquefied natural gas (LNG) transported by sea [2]. This favours a rise in global demand for LNG and also an increase in regasification capacity through the installation of new onshore or offshore import terminals such as Floating Storage Regasification Units (FSRUs). Specifically, FSRUs have experienced rapid growth in recent years and now account for more

than 25 % of existing regasification terminals [3]. In view of the new construction of FSRUs, this percentage will continue to increase and will be reinforced if the commitments announced by several European countries to install regasification vessels on their coasts in order to reduce dependence on Russian gas are fulfilled. The LNG transport involves liquefaction of the hydrocarbon at slightly above atmospheric pressure and at a temperature of approximately -162 °C for storage in the tanks of LNG carriers [4]. However, LNG must be regasified for pipeline distribution of the hydrocarbon to end users [5]. Regasification of LNG involves two basic thermodynamic processes: the increase of the pressure above the critical value and the increase of the temperature to a value of approximately 10 °C. Therefore, seawater is usually at a suitable temperature to be used as a heat source for the regasification process (open loop system) [6]. However, if the ambient temperature is too low or if the authorities prohibit the use of seawater, it is necessary to burn NG and transfer the combustion energy to the LNG by means of an intermediate fluid (closed loop system). Thus, while open loop systems only need electrical power for seawater supply, closed loop systems use NG combustion to increase the temperature of the LNG, leading to higher CO_2 emissions associated with the regasification process.

Regarding CO_2 emissions regulations in the maritime sector, the International Maritime Organization (IMO) added in 2011 a new chapter to MARPOL Annex VI, Chapter 4 - Regulations on energy efficiency for ships (recently renamed as Regulations on the carbon intensity of international shipping) [7]. The regulations contained in this chapter entered into force at the beginning of 2013 and entail the requirement to determine the Energy Efficiency Design Index (EEDI) for most new vessels, whose value must be lower than the limit set by IMO depending on the vessel type and cargo capacity. Considering the growing global interest in reducing CO_2 emissions, IMO resolution MEPC.328(76) recently introduced two additional measures: the Energy Efficiency Index of Existing Ships (EEXI) and the Carbon Intensity Indicator (CII) [8]. While the EEXI is an index similar to the EEDI, but for all existing vessels, the CII is an operational indicator that evaluates the vessel's annual emissions. However, the IMO regulations so far have the disadvantage that they only are applicable to vessels dedicated to cargo transport and does not consider those that operate on a stationary basis, such as FSRUs [9]. Therefore, these indices and indicators do not allow the CO_2 emissions of the regasification process in an FSRU to be determined, nor do they allow the regasification systems implemented to be evaluated.

Most of the systems installed at regasification terminals are not designed to recover the LNG cold energy previously acquired in the liquefaction process and, consequently, it is released directly into the environment. This has led the scientific community to investigate the utilisation of LNG cold energy, especially its application in power generation through power cycles [10,11]. Among the cycles considered by researchers, the Organic Rankine Cycle (ORC) is the most frequent and has been the first to be applied in onshore regasification terminals, where LNG is used as a sink [4]. As far as offshore regasification is concerned, there is currently no system installed on board FSRUs that exploits LNG cold energy for power generation [12]. However, companies in the sector, MOL and DSME, have developed a regasification system with simple ORC for FSRUs [13].

Studies on the utilisation of cold energy by ORC focus on the selection of working fluids, cycle architectures and integration of waste or renewable heat sources. The number of papers is very large and the main contributions of authors are reported in recent reviews such as in [10,12,14–16]. In the aforementioned reviews, it can be seen that the number of investigations on the application of zeotropic mixtures as working fluid is lower than those with pure fluids, despite the fact that this type of mixtures can improve the power generated by ORCs [17,18]. Regarding works dealing with the utilisation of cold energy on board FSRUs, the number of

publications is rather limited. The main studies related to regasification vessels are presented below.

Regarding the integration of simple ORC in open-loop regasification systems, Yao et al. [19] study the thermodynamic performance (first and second law) considering several working fluids and conclude that propane is the best candidate. Based on this work, the following papers propose more complex and efficient systems than the simple ORC, which can be classified according to the type of configuration studied, i.e., series ORCs or cascade ORCs. Starting with the first type of arrangement, Lee et al. [20] evaluate up to two stages in series and consider the integration of waste heat from the exhaust gas of FSRU engines into the cold energy utilisation power generation system. The two-stage ORC with exhaust gases achieves a clear reduction in seawater use and improves electrical power production compared to simple ORC or conventional two-stage ORC. Next, Yoon-Ho [21] performs energy, exergy and economic analysis of up to three stages in series and considers the integration of a partial expander. The latter component expands part of the regasified NG to supply the fuel gas consumed in the engines. Regarding cascaded ORCs, Yao et al. [22] evaluate two three-stage configurations, while Xu and Lin [23] propose two power cycles: a novel three-stage and a four-stage configuration. Based on the results obtained from these studies, cascade configurations allow higher exergy efficiencies to be achieved than cycles in series. The papers mentioned so far use pure working fluids in the ORC stages. Regarding the application of zeotropic mixtures as working fluid, only Yoon-Ho [24] considers their use in the thermo-economic assessment of two power cycles: simple ORC and two-stage ORC in series. In the study, ethane-propane mixture is used as the working fluid in the simple ORC and in the low-temperature stage of the two-stage ORC. In both systems, the zeotropic mixture significantly increases the electric power generation in comparison with pure fluids.

In summary, the limited research on LNG cold energy utilisation in FSRUs focuses on open loop regasification systems with both series and cascade configurations of ORCs and the possible integration of waste heat sources into the process such as engine exhaust gases. Regarding the working fluids used, these are mostly pure, with ethane and propane offering the best results, although it has been shown that the zeotropic ethane/propane mixture is able to improve the electrical energy production of the power cycle.

None of the above-mentioned studies takes into consideration the effect of integrating the ORC into the FSRU's electrical power balance, i.e., the reduction of power generation on the dual fuel (DF) engines and, consequently, the reduction of fuel consumption and greenhouse gas (GHG) emissions. In addition, the implementation of LNG open power cycle (OC) in combination with ORC has not been considered in these studies. Unlike the ORC, which uses its own working fluid, the OC is a transcritical cycle with NG as the working fluid. Specifically, in this cycle, part of the regasified NG, which is in a supercritical state, is expanded in a turbine and subsequently condensed with the cold energy of the LNG supplied to the regasification system [4,25]. The ORC-OC system has been previously introduced in [26] with the aim of achieving zero carbon emissions during the regasification process of the FSRU. However, in order to meet the electrical power demand, i.e., to avoid the use of dual fuel (DF) engines, complex ORC-OC systems with at least two stages need to be installed. Therefore, this previous study covers the thermo-economic analysis of two-stage and three-stage ORC-OC systems (2ORC-OC and 3ORC-OC), but not the simple ORC-OC. Furthermore, it does not compare from a thermodynamic, economic and environmental point of view the ORC-OC system with the simple ORC, when the latter is the most basic and conventional power cycle for cold energy utilisation considered in the scientific literature.

Therefore, taking into account the gaps in the existing literature, this study performs the energy, exergy, economic and environmental analysis of an open loop regasification system

that combines a simple ORC with an OC (ORC-OC) to achieve a significant reduction of GHG emissions in FSRUs. In the proposed system, an ethane/propane mixture is considered as the working fluid of the ORC to improve the production of electrical energy. The ORC-OC system is compared from energy, exergy, economic and environmental points of view with the simple ORC system considered by researchers in previous publications. Finally, the systems analysed in this study are compared with conventional regasification systems installed on board FSRUs and other systems proposed in previous work by the authors.

2. System description

This section describes the studied configurations: the ORC-OC system and the ORC system. Fig. 1 shows the simplified scheme of the ORC-OC system with the main components of the OC, turbine and condenser, represented by dashed lines. The ORC system presents the same basic layout, but without the OC equipment. The systems are evaluated on a model FSRU with a dual fuel diesel electric (DFDE) propulsion system previously presented in [27], which is more efficient than the conventional steam turbine system [28]. Tables A. 1 and A. 2 include the main characteristics of the vessel and the specific fuel consumptions of the DF engines, respectively. Next, the regasification systems studied are described based on the trajectories followed by the LNG and boil off gas (BOG), starting with the ORC system shown in Fig. 2.

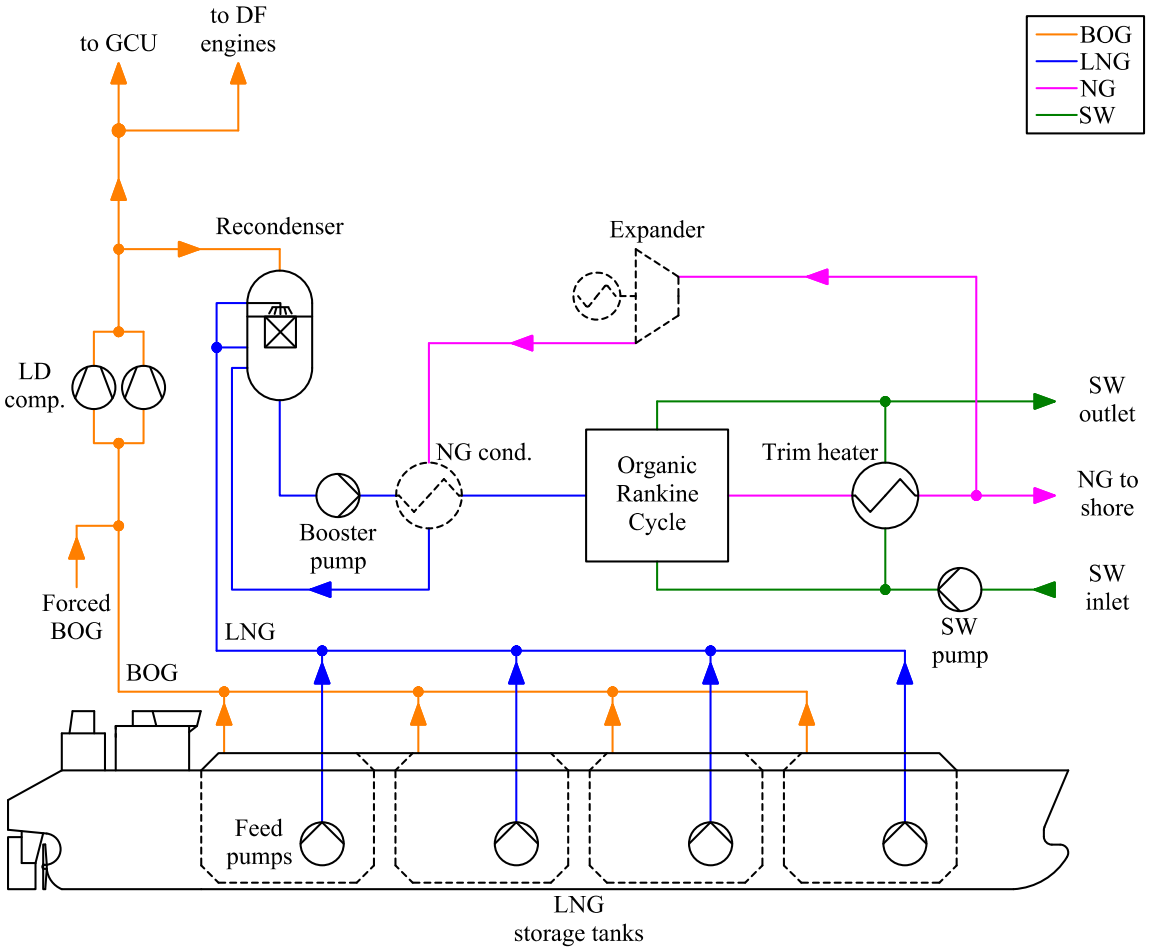

Fig. 1 Simplified scheme of the ORC-OC regasification system.

Fig. 2a shows the processes related to LNG supply and BOG handling of the ORC system. The LNG stored in the cargo tanks is discharged by the feed pump (P-1) to the recondenser (R). In the inlet line to this component, the LNG decreases the pressure in the valve (V-1). The LNG then exits the bottom of the recondenser and is directed to the booster pump (P-2) to increase the pressure to the value required for pipeline distribution of the hydrocarbon. The high pressure LNG increases the temperature in the condenser of the OC (CD-1) and subsequently in the condensation process of the ORC working fluid. As for the management of the BOG coming from the storage tank, it is mixed with the BOG produced in the forced vaporiser (FV). This heat exchanger vaporises part of the LNG cargo and is used when it is not possible to satisfy the gas fuel demand of the DF engines with the natural BOG produced in the tank. In any case, the BOG must be pre-cooled to increase the pressure up to about 6 bar in the low duty (LD) compressor. Specifically, in the mixer (MX) the temperature is reduced to -120 °C and then the condensables are removed in the phase separator (S). The cooling process of the BOG in the mixer is carried out by mixing a small amount of LNG supplied by the fuel gas pump which is located in the storage tank. In case of using the forcing vaporizer, the above-mentioned pump is responsible for supplying the LNG to this heat exchanger. Part of the high pressure BOG from the low duty compressor is consumed by the DF engines and conditioned in the natural gas aftercooler/heater (AC/NGH), while the remaining BOG flows to the recondenser through the valve (V-2). If the BOG exceeding the consumption of the DF engines cannot be treated in the recondenser, it is necessary to burn it in the Gas Combustion Unit (GCU). With regard to the regasification process, Fig. 2b shows the integration of the simple ORC. This cycle consists of a pump (P-3) to increase the pressure of the working fluid, a vaporiser (VP-1) that exchanges heat with the seawater and a condenser (CD-1) that exploits the LNG cold energy. The seawater is supplied by the pump (P-4) to the ORC and the trim heater (TH). In the latter heat exchanger, the NG reaches the appropriate temperature for export by pipeline.

The ORC-OC regasification system is practically identical to the one described above, however, there are some differences according to the integration of the OC as shown in Fig. 3. In this system, the LNG coming from the booster pump increases the temperature in the OC condenser (CD-1) before entering the ORC condenser (CD-2) and trim heater (TH). In the latter component, the NG temperature is sufficiently increased to export the hydrocarbon to shore. However, part of the regasified NG flow rate is recirculated for use as the OC working fluid: the fluid is expanded in the turbine (T-1) and then condensed in CD-1. In this way, the recirculated NG flow rate in liquid state is reintroduced to the regasification process in the recondenser.

Unlike OC, the ORC working fluid is independent of the LNG composition, therefore, the ethane/propane mixture can be modified to maximise the power produced in the latter cycle. By adjusting the ethane/propane composition, the temperature profiles in the heat exchange processes with LNG are closer, because there is a temperature glide in the phase change process (see Fig. 4).

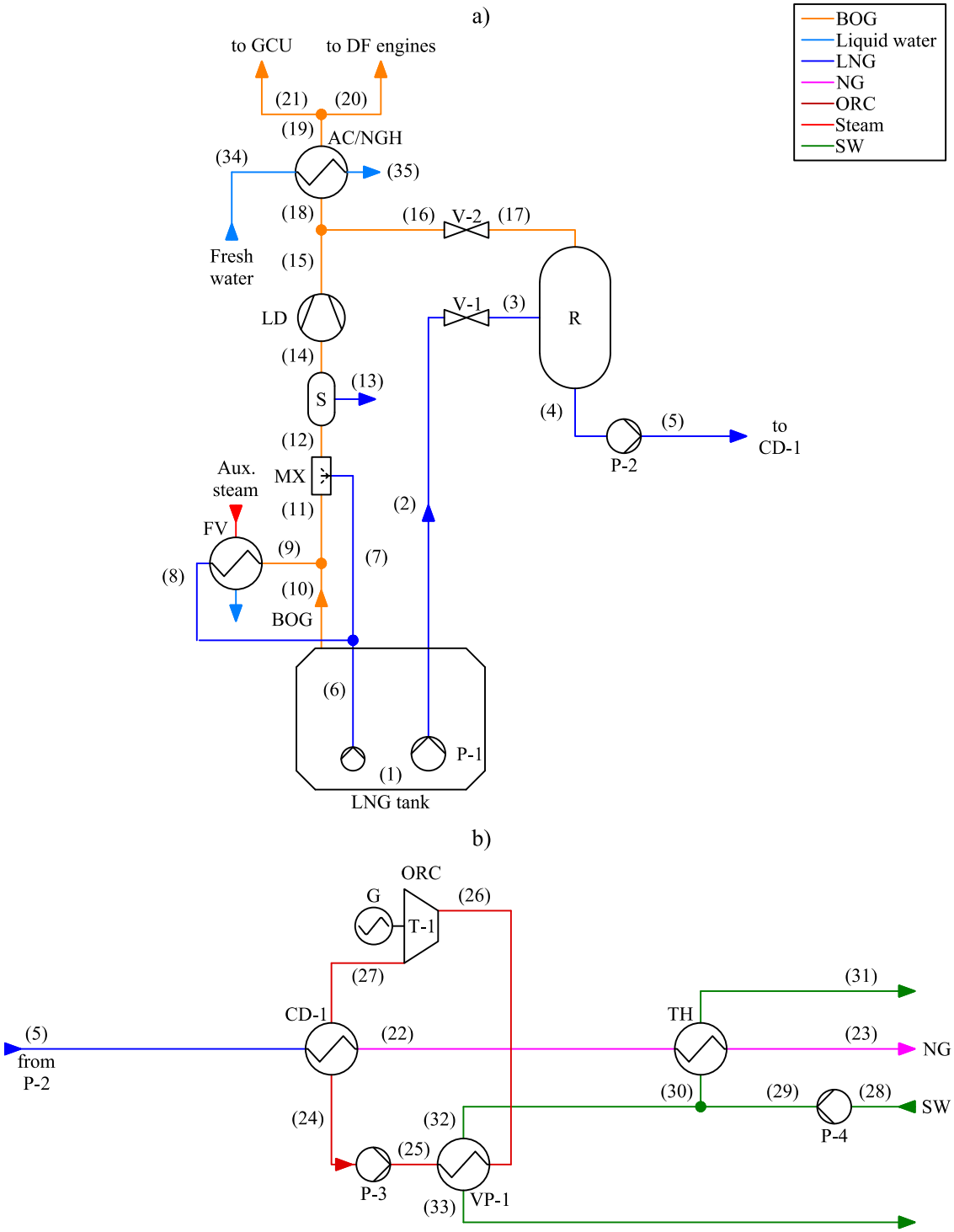

Fig. 2 Diagram of the ORC regasification system: a) BOG handling and LNG feed systems, b) simple ORC arrangement.

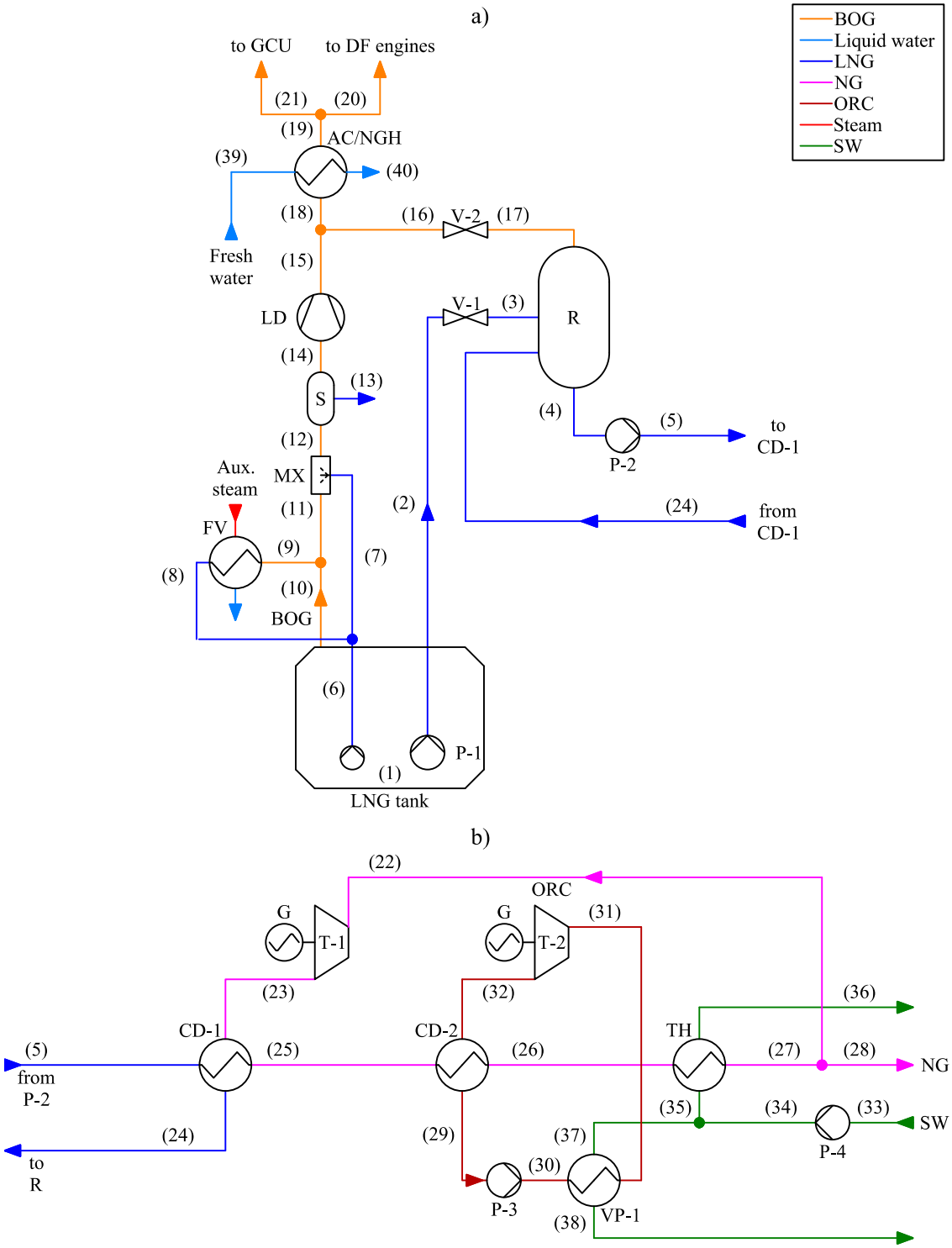

Fig. 3 Diagram of the ORC-OC regasification system: a) BOG handling and LNG feed systems, b) ORC-OC arrangement.

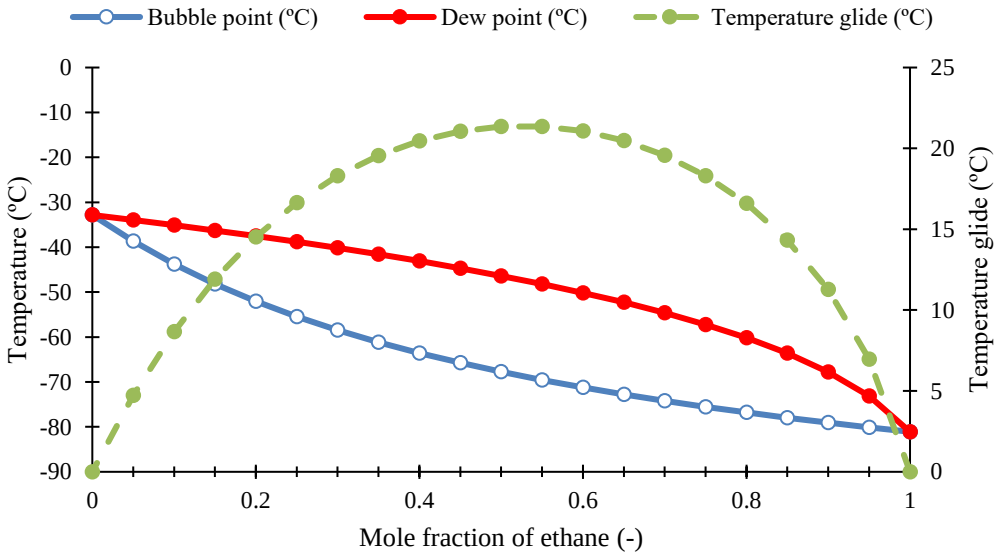

Fig. 4 Vapour-liquid phase change temperatures of the working fluid as a function of the ethane/propane composition.

3. Mathematical modelling

The regasification systems are modelled in Aspen HYSYS using the Peng Robinson equation of state to calculate the properties of the NG and ORC working fluid. As for seawater, this fluid is considered as pure water and therefore the IAPWS-IF97 package is used to determine the thermodynamic properties. The study addresses the effect of LNG composition on electric power generation, so two compositions are considered: pure methane and LNG composition measured on board an FSRU (see Table A. 3). The first one is treated as the LNG reference composition with a net calorific value of 49 500 kJ/kg.

The following subsections explain the methodology carried out in the energy, energy, economic and environmental analyses of the systems.

3.1 Energy analysis

The energy analysis is based on the principle of conservation of energy, i.e., the first law of thermodynamics. Thus, the energy balances under adiabatic conditions for each component of the regasification systems, ignoring kinetic and potential energy effects, are shown in Table 1 as well as the mass balances.

With regard to the heat transfer from the environment to the LNG storage tanks, the BOG to be extracted ($\dot{m}_{\mathrm{BOG}}$) is defined as [9,29]:

$$\dot{m}_{\mathrm{BOG}} = \dot{m}_{\mathrm{BOG,n}} - \frac{v_{\mathrm{LNG}}}{v_{\mathrm{BOG}}}\left(\dot{m}_{\mathrm{LNG}} + \dot{m}_{\mathrm{BOG,n}}\right) = \frac{BOR\, V_{\mathrm{tk}}}{v_{\mathrm{LNG}}} - \frac{v_{\mathrm{LNG}}}{v_{\mathrm{BOG}}}\left(\dot{m}_{\mathrm{LNG}} + \frac{BOR\, V_{\mathrm{tk}}}{v_{\mathrm{LNG}}}\right) \quad (1)$$

where $\dot{m}_{\mathrm{BOG,n}}$ is the natural BOG mass flow rate generated by the heat input, BOR is the boil-off rate, V_{tk} is the LNG storage capacity, $\dot{m}_{\mathrm{LNG}}$ is the LNG mass flow rate extracted from the storage tanks and v_{LNG} and v_{BOG} are the specific volume of LNG and BOG, respectively.

Table 1 Balance equations for components of the regasification systems analysed

Component	Mass	Energy
Pumps and compressors	$\dot{m}_i = \dot{m}_o$	$\dot{W}_{\text{pump/comp}} = \dot{m}(h_o - h_i)$
Turbines	$\dot{m}_i = \dot{m}_o$	$\dot{W}_{\text{turb}} = \dot{m}(h_i - h_o)$
Valves	$\dot{m}_i = \dot{m}_o$	$h_i = h_o$
Mixer and recondenser	$\sum_i \dot{m}_i = \dot{m}_o$	$\sum_i \dot{m}_i h_i = \dot{m}_o h_o$
Phase separator	$\dot{m}_i = \sum_o \dot{m}_o$	$\dot{m}_i h_i = \sum_o \dot{m}_o h_o$
Heat exchangers	$\sum_i \dot{m}_i = \sum_o \dot{m}_o$	$\sum_i \dot{m}_i h_i = \sum_o \dot{m}_o h_o$

Determining the electrical demand of the FSRU involves calculating the electrical power consumed by the pumps and compressors in the regasification system. The electrical power consumed by each pump or compressor ($\dot{W}_{\text{el,pump/comp}}$) is defined by the electromechanical efficiency ($\eta_{\text{el,m}}$) as follows:

$$\dot{W}_{\text{el,pump/comp}} = \frac{\dot{W}_{\text{pump/comp}}}{\eta_{\text{el,m}}} \tag{2}$$

Thus, the electric power demand in the FSRU ($\dot{W}_{\text{el,FSRU}}$) can be calculated as:

$$\dot{W}_{\text{el,FSRU}} = \dot{W}_{\text{el,b}} + \sum \dot{W}_{\text{el,pump}} + \sum \dot{W}_{\text{el,comp}} \tag{3}$$

where $\dot{W}_{\text{el,b}}$ represents the electric power demand of the vessel's auxiliary services with a value of 2050.9 kW [27].

The electric power to be generated by the engines ($\dot{W}_{\text{el,eng}}$) must be equal to the electric power demand of the FSRU considering the power generation of turbines as the following equation implies:

$$\dot{W}_{\text{el,eng}} = \dot{W}_{\text{el,FSRU}} - \sum \dot{W}_{\text{turb}} \eta_{\text{alt}} \tag{4}$$

where η_{alt} is the efficiency of each turbine alternator.

The total power delivered by the DF engines ($\dot{W}_{\text{eng}}$) is calculated with Eq. (5) and distributed between two engines: a 6L50DF and a 12V50DF. The load sharing is done by minimising the fuel consumption according to Table 2.

$$\dot{W}_{\text{eng}} = \frac{\dot{W}_{\text{el,eng}}}{\eta_{\text{alt}}} \tag{5}$$

The specific energy consumption of the NG ($b_{\text{BOG}(i)}$) and pilot diesel oil (DO) ($b_{\text{DO}(i)}$) depends on the power developed by the engine ($\dot{W}_{\text{eng}(i)}$). These parameters are calculated with third order polynomial regressions of the data in Table A. 2. Therefore, the mass flow rates of both fuels consumed ($\dot{m}_{\text{BOG}(i)}$ and $\dot{m}_{\text{DO}(i)}$) are:

$$\dot{m}_{\text{BOG}(i)} = \frac{b_{\text{BOG}(i)} \dot{W}_{\text{eng}(i)}}{h_{\text{LHV,BOG}}} \tag{6}$$

$$\dot{m}_{\mathrm{DO}(i)} = \frac{b_{\mathrm{DO}(i)} \dot{W}_{\mathrm{eng}(i)}}{h_{\mathrm{LHV,DO}}} \quad (7)$$

where $h_{\mathrm{LHV,BOG}}$ is the NG net calorific value, and $h_{\mathrm{LHV,DO}}$ is the DO net calorific value.

Table 2 Engines load sharing as a function of the power delivered [27]

Conditions	Load sharing	
	6L50DF	12V50DF
$\dot{W}_{\mathrm{eng}} < 80\ \%\ \dot{W}_{\mathrm{6L,max}}$ (1)	$\dot{W}_{\mathrm{eng}}$	-
$80\ \%\ \dot{W}_{\mathrm{6L,max}} < \dot{W}_{\mathrm{eng}} < 80\ \%\ \dot{W}_{\mathrm{12V,max}}$ (2)	-	$\dot{W}_{\mathrm{eng}}$
$80\ \%\ \dot{W}_{\mathrm{6L,max}} < \dot{W}_{\mathrm{eng}}$ $\dot{W}_{\mathrm{eng}} < 12.5\ \%\ \dot{W}_{\mathrm{6L,max}} + 80\ \%\ \dot{W}_{\mathrm{12V,max}}$	$12.5\ \%\ \dot{W}_{\mathrm{6L,max}}$	$\dot{W}_{\mathrm{eng}} - \dot{W}_{\mathrm{6L}}$
$12.5\ \%\ \dot{W}_{\mathrm{6L,max}} + 80\ \%\ \dot{W}_{\mathrm{12V,max}} < \dot{W}_{\mathrm{eng}}$	$\dot{W}_{\mathrm{eng}} - \dot{W}_{\mathrm{12V}}$	$80\ \%\ \dot{W}_{\mathrm{12V,max}}$

Notes: (1) Maximum engine power of 6L50DF ($\dot{W}_{\mathrm{6L,max}}$). (2) Maximum engine power of 12V50DF ($\dot{W}_{\mathrm{12V,max}}$).

The total consumption of each fuel ($\dot{m}_{\mathrm{BOG}}$ and $\dot{m}_{\mathrm{DO}}$) can be calculated as:

$$\dot{m}_{\mathrm{BOG}} = \sum \dot{m}_{\mathrm{BOG}(i)} \quad (8)$$

$$\dot{m}_{\mathrm{DO}} = \sum \dot{m}_{\mathrm{DO}(i)} \quad (9)$$

Finally, the specific energy consumption of the FSRU (b_{FSRU}) is determined with the following equation:

$$b_{\mathrm{FSRU}} = \frac{\dot{m}_{\mathrm{BOG}} h_{\mathrm{LHV,BOG}} + \dot{m}_{\mathrm{DO}} h_{\mathrm{LHV,DO}}}{\dot{m}_{\mathrm{NG}}} \quad (10)$$

The main parameters assumed in the study of the regasification systems are presented in Table A. 4.

3.2 Exergy analysis

The irreversibilities associated with the different components of regasification systems result in the destruction of useful work (exergy). In this study, the specific exergy flow rate of a material stream (e) is defined in Eq. (11) considering two terms: the physical exergy (e^{ph}) and the chemical exergy (e^{ch}).

$$e = e^{\mathrm{ph}} + e^{\mathrm{ch}} \quad (11)$$

However, for a proper definition of the FSRU efficiency, the physical exergy term of NG is split into thermal exergy (e^{th}) and mechanical exergy (e^{p}) as follows [30]:

$$e^{\mathrm{ph}} = h - h_0 - T_0(s - s_0) \quad (12)$$

$$e^{\mathrm{th}} = e^{\mathrm{ph}}(T, p) - e^{\mathrm{ph}}(T_0, p) \quad (13)$$

$$e^{\mathrm{p}} = e^{\mathrm{ph}}(T_0, p) - e^{\mathrm{ph}}(T_0, p_0) \quad (14)$$

where the terms with subscript 0 are the values of the same properties at the dead state.

In the analysis of the regasification systems, it is only necessary to determine the chemical exergies of NG and DO with Eqs. (15) and (16), respectively. These equations calculate the

chemical exergy as function of the net calorific value and an exergy factor of the fuel. The exergy factors assumed for BOG (φ_{BOG}) and DO (φ_{DO}) are 1.04 and 1.07, respectively [31].

$$e_{\mathrm{BOG}}^{\mathrm{ch}} = \varphi_{\mathrm{BOG}} h_{\mathrm{LHV,BOG}} \tag{15}$$

$$e_{\mathrm{DO}}^{\mathrm{ch}} = \varphi_{\mathrm{DO}} h_{\mathrm{LHV,DO}} \tag{16}$$

After defining the exergies needed to perform the analysis of the systems, the exergy destroyed (exergy balance) and exergy efficiency of components of the regasification systems are determined with the equations in Table 3.

Table 3 Balance equations for components of the regasification systems analysed

Component	Exergy destruction	Exergy efficiency
Pumps and compressors	$\dot{I}_{\mathrm{pump/comp}} = \dot{W}_{\mathrm{pump/comp}} - \dot{m}(e_o - e_i)$	$\eta_{\mathrm{ex,pump/comp}} = \frac{\dot{m}(e_o - e_i)}{\dot{W}_{\mathrm{pump/comp}}}$
Turbines	$\dot{I}_{\mathrm{turb}} = \dot{m}(e_i - e_o) - \dot{W}_{\mathrm{turb}}$	$\eta_{\mathrm{ex,turb}} = \frac{\dot{W}_{\mathrm{turb}}}{\dot{m}(e_i - e_o)}$
Valves	$\dot{I}_{\mathrm{valve}} = \dot{m}(e_i - e_o)$	-
Mixer and recondenser	$\dot{I}_{\mathrm{MX/R}} = \sum_i \dot{m}_i e_i - \dot{m}_o e_o$	$\eta_{\mathrm{ex,MX/R}} = \frac{[\dot{m}(e_o - e_i)]_{\mathrm{product}}}{[\dot{m}(e_i - e_o)]_{\mathrm{supply}}}$
Heat exchangers	$\dot{I}_{\mathrm{HE}} = \sum_i \dot{m}_i e_i - \sum_o \dot{m}_o e_o$	$\eta_{\mathrm{ex,HE}} = \frac{[\dot{m}(e_o - e_i)]_{\mathrm{product}}}{[\dot{m}(e_i - e_o)]_{\mathrm{supply}}}$
ORC	$\dot{I}_{\mathrm{ORC}} = (\dot{E}_{\mathrm{LNG}} - \dot{E}_{\mathrm{NG}}) + (\dot{E}_{\mathrm{SW,in}} - \dot{E}_{\mathrm{SW,out}}) - \dot{W}_{\mathrm{ORC}}$	$\eta_{\mathrm{ex,ORC}} = \frac{\dot{W}_{\mathrm{ORC}} + (\dot{E}_{\mathrm{SW,in}} - \dot{E}_{\mathrm{SW,out}})}{(\dot{E}_{\mathrm{LNG}} - \dot{E}_{\mathrm{NG}})}$

Finally, the exergy efficiency of the FSRU ($\eta_{\mathrm{ex,FSRU}}$) is defined as:

$$\eta_{\mathrm{ex,FSRU}} = \frac{(\dot{E}_{\mathrm{NG}}^{\mathrm{p}} + \dot{E}_{\mathrm{cond}}^{\mathrm{p}}) - (\dot{E}_{\mathrm{LNG}}^{\mathrm{p}} + \dot{E}_{\mathrm{BOG}}^{\mathrm{p}})}{\dot{E}_{\mathrm{DO}} + (\dot{E}_{\mathrm{LNG}}^{\mathrm{ch}} + \dot{E}_{\mathrm{BOG}}^{\mathrm{ch}}) - (\dot{E}_{\mathrm{NG}}^{\mathrm{ch}} + \dot{E}_{\mathrm{cond}}^{\mathrm{ch}}) + (\dot{E}_{\mathrm{LNG}}^{\mathrm{th}} + \dot{E}_{\mathrm{BOG}}^{\mathrm{th}}) - (\dot{E}_{\mathrm{NG}}^{\mathrm{th}} + \dot{E}_{\mathrm{cond}}^{\mathrm{th}})} \tag{17}$$

where $\dot{E}_{\mathrm{DO}}$ is the pilot DO exergy flow rate supplied to the DF engines. In this equation, the exergy flow rates of the LNG and BOG leaving the cargo storage tanks are represented with subscripts LNG and BOG, while those for regasified NG and condensables from the mist separator are represented with NG and cond subscripts.

3.3 Economic analysis

The economic analysis of regasification systems is carried out by considering the components which constitute the regasification modules. Each module is composed of two booster pumps and the components involved in the regasification process, including those related to intermediate fluids such as ORC. In the study, the FSRU is considered to have 3 regasification modules with a total maximum capacity of 750 mmscfd (see Table A.1). As FSRUs are usually designed to operate continuously at the baseload regasification capacity (500 mmscfd), the economic analysis of each of the regasification systems is performed considering two modules with the cold energy utilisation system and the third module with a conventional regasification system. Specifically, the third module consists of an open-loop propane regasification system previously analysed in [27]. The method used in the economic assessment has been applied in [27] and the equations are presented below.

The total cost rate of a regasification system ($\dot{C}_{\mathrm{tot}}$) can be calculated with the following equations:

$$\dot{C}_{\mathrm{tot}} = \dot{C}_{\mathrm{f,tot}} + \dot{Z}_{\mathrm{tot}}^{\mathrm{CI}} + \dot{Z}_{\mathrm{tot}}^{\mathrm{OM}} \tag{18}$$

$$\dot{Z}_{\mathrm{tot}}^{\mathrm{CI}} + \dot{Z}_{\mathrm{tot}}^{\mathrm{OM}} = \frac{Z_{\mathrm{tot}}^{\mathrm{CI}}(\gamma_{\mathrm{OM}} + \beta_{\mathrm{CRF}})}{\tau} \tag{19}$$

where $\dot{C}_{\mathrm{f,tot}}$ is the cost rate associated with fuels, $\dot{Z}_{\mathrm{tot}}^{\mathrm{CI}}$ is the capital investment cost rate, $\dot{Z}_{\mathrm{tot}}^{\mathrm{OM}}$ is the operation and maintenance cost rate, $Z_{\mathrm{tot}}^{\mathrm{CI}}$ is the capital investment cost of the regasification system, γ_{OM} is the operation and maintenance factor, τ is the annual operating hours and β_{CRF} is the capital recovery factor calculated in Eq. (20) based on the annual interest (i) and the estimated lifetime of the regasification system (n) [32].

$$\beta_{\mathrm{CRF}} = \frac{i(1+i)^n}{(1+i)^n - 1} \tag{20}$$

In order to compare the regasification systems evaluated in this study with those considered in previous works, the CEPCI is used to update the capital investment cost of each system to 2019. This is achieved with the following equation:

$$Z_{\mathrm{tot}}^{\mathrm{CI}} = \frac{CEPCI_{2019}}{CEPCI_{\mathrm{March,2018}}} (FCI)_{\mathrm{March,2018}} \tag{21}$$

where FCI is the fixed capital investment, often referred to as total project cost. This term is calculated from the programmes contained in the AspenONE Suite. Specifically, the regasification systems are modelled in Aspen HYSYS, the heat exchangers are designed in Aspen EDR and, finally, the APEA determines the total project cost. The cost basis date of the latter programme is March 2018 [33].

Table 4 lists the main economic parameters assumed in the study of regasification systems.

Table 4 Economic analysis parameters

Parameter	Value
γ_{OM}	3 % [34]
i	12 % [32]
n	20 years [21]
τ	8000 hours
$CEPCI_{\mathrm{March,2018}}$	588 [35]
$CEPCI_{2019}$	607.5 [35]

3.4 Environmental analysis

The environmental analysis of the regasification systems is performed through the Energy Efficiency Regasification Indicator (EERI) and the Carbon Footprint Regasification Indicator (CFRI). The EERI determines the CO_2 emissions resulting from fuel consumption during the regasification process onboard the FSRU, while the CFRI further considers the effects of CO_2 capture systems (if installed) and methane unburned from DF engines (methane slip).

The EERI is determined as follows [9]:

$$EERI\left(\frac{\mathrm{g_{CO_2}}}{\mathrm{MJ}}\right) = \frac{\sum_j \dot{m}_j c_{\mathrm{F}j}}{\dot{m}_{\mathrm{NG}}(h_{\mathrm{NG}} - h_{\mathrm{LNG}})} \tag{22}$$

where $\dot{m}_j$ is the fuel mass flow rate, C_{Fj} is the non-dimensional conversion factor between fuel consumption and CO_2 emissions (g CO_2/g fuel), h_{NG} is the specific enthalpy of the regasified NG and h_{LNG} is the specific enthalpy of saturated liquid at the temperature of the LNG contained in the storage tanks with the same composition as the regasified NG.

Considering that the systems studied do not involve CO_2 capture processes, the equation of CFRI can be simplified as [9]:

$$CFRI\left(\frac{\mathrm{g_{CO_2e}}}{\mathrm{MJ}}\right) = \frac{\sum_j \dot{m}_j C_{\mathrm{F}j} + \dot{m}_{\mathrm{CH_4}}\left(GWP_{\mathrm{CH_4}} - C_{\mathrm{F,CH_4}}\right)}{\dot{m}_{\mathrm{NG}}\left(h_{\mathrm{NG}} - h_{\mathrm{LNG}}\right)} \quad (23)$$

where $\dot{m}_{\mathrm{CH_4}}$ is the mass flow rate of methane in DF engine exhaust gases, $GWP_{\mathrm{CH_4}}$ is the global warming potential (GWP) of methane and $C_{\mathrm{F,CH_4}}$ is the non-dimensional conversion factor between methane and CO_2 emissions.

The parameters assumed to calculate the EERI and CFRI of the regasification systems evaluated are presented in Table 5.

Table 5 Environmental analysis parameters

Parameter	Value
$C_{\mathrm{F,CH_4}}$	2.750 [36]
$C_{\mathrm{F,DO}}$	3.206 [36]
100-years $GWP_{\mathrm{CH_4}}$	28 [37]
Methane slip	5.5 g/kW h [38,39]

4. Results and discussion

The results obtained from the thermodynamic, economic and environmental analysis of the regasification systems are discussed in the following subsections. Specifically, section 4.1 presents the results related to the effect of both the working fluid and LNG composition on the power to be generated by the DF engines during the regasification process of the FSRU. After obtaining the optimal compositions, section 4.2 gives the energy, exergy and environmental results of the systems, while section 4.3 gives the economic results. Finally, section 4.4 compares the regasification systems analysed in this study with systems evaluated in previous works.

4.1 Effect of working fluid composition

Fig. 5 shows the effect of the working fluid composition in the ORC regasification system on the electrical power to be produced by the DF engines (required power), simulating the LNG both as pure methane and with the composition of Table A. 3. Specifically, in the case of pure methane, it can be seen how a molar composition ratio of 76:24 ethane/propane is able to reduce the required power by 64.65 % with respect to pure propane (45.84 % if ethane is used as a reference). However, the effect of LNG composition on this parameter as the ethane content increases is relevant. While in the case of pure propane the difference in the required power for both LNG compositions is only 0.85 %, this value increases to a maximum of 66.66 % if the ethane/propane molar composition is 76:24. Thus, for the LNG in Table A. 3, the optimal working fluid composition (75:25 ethane/propane) reduces the power requirement for pure propane by 41.61 % (24.76 % for pure ethane).

In the ORC-OC regasification system, the NG mass flow rate recirculated through the OC influences the optimal composition of the ORC working fluid. For the optimisation of the ORC-

OC system, the simulation is started with the optimal composition of the ORC system and then the OC flow rate is increased with a step of 0.01 kg/s until the minimum required power value is reached. Finally, the composition of the ORC working fluid is adjusted. Table 6 presents the optimal compositions of the working fluids for the regasification systems studied, including the ORC system with pure propane (P-ORC), while Fig. 6 gives the required power for each system. Based on the results obtained, the ORC-OC system reduces the required power by 84.35 and 55.73 % with respect to the P-ORC and ORC systems, respectively. However, these values decrease to 73.37 and 54.40 % for the LNG in Table A. 3. It should be noted that the maximum NG flow rate through the OC is more than double for this real composition compared to pure methane.

The composition of the LNG is undoubtedly a factor to be considered when determining the power generated by the cycles, however, the composition depends on the origin of the hydrocarbon. Therefore, the following sections present the results of the three regasification systems with the optimal values obtained for pure methane.

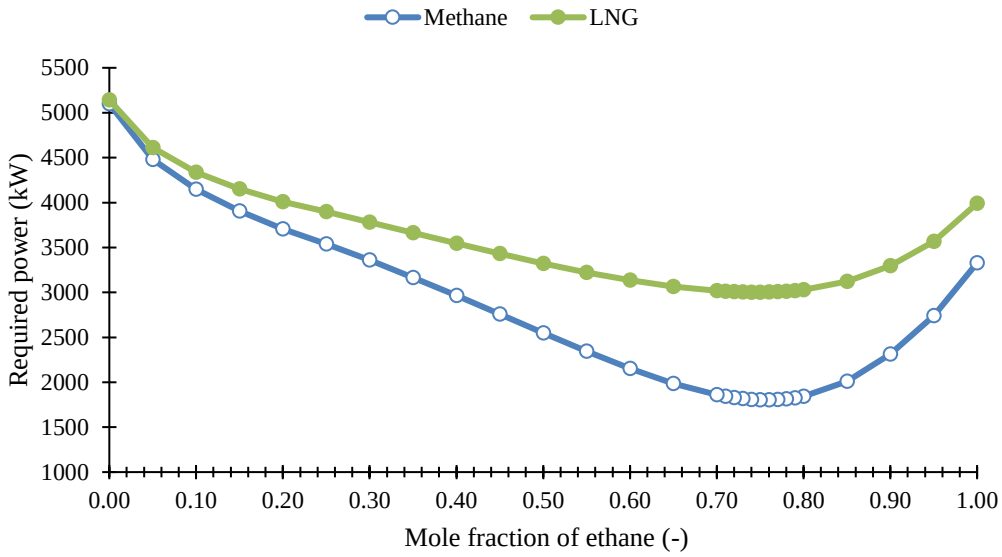

Fig. 5 Power required in the ORC system as a function of LNG and working fluid (ethane/propane mixture) compositions.

Table 6 Optimal working fluid composition and OC mass flow for each system as a function of LNG composition

Cycle	Working fluid (ethane mole fraction)		OC mass flow rate (kg/s)	
	Methane	LNG	Methane	LNG
P-ORC	0.00	0.00	-	-
ORC	0.76	0.75	-	-
ORC-OC	0.73	0.74	9.30	19.38

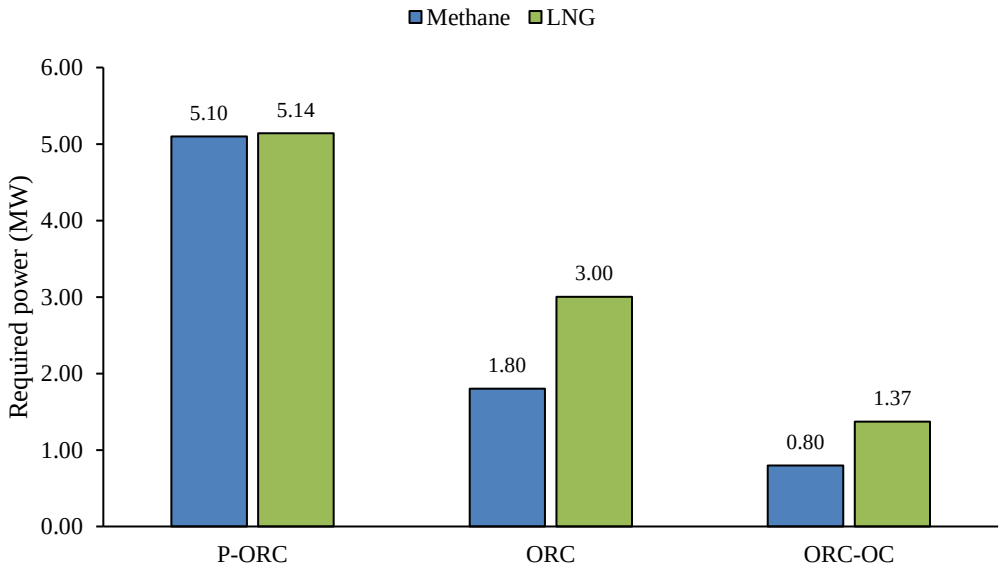

Fig. 6 Power required by each system as a function of LNG composition with optimal working fluid compositions

4.2 Thermodynamics and environment

The main thermodynamic properties of the P-ORC, ORC and ORC-OC states are given in Tables A. 5, A. 6 and A. 7, while the compositions are presented in Tables A. 8, A. 9 and A. 10. The main energy, exergy and environmental results for the three systems are shown in Table 7. Of the systems evaluated, the ORC-OC system has the highest electrical power demand, but also achieves the highest output through the ORC and OC turbines. Thus, the ORC-OC system reduces the specific energy consumption of the FSRU by 76.97 and 59.54 % compared to the P-ORC and ORC systems, respectively. In relation to the exergy results, the ORC-OC system presents the lowest exergy input and the lowest exergy destroyed for the same regasification capacity of the evaluated systems, becoming the system with the highest exergy efficiency. The EERI results are similar to those obtained in the energy analysis for specific energy consumption. Regarding the CFRI calculation, the ORC-OC system reduces CO_2e emissions by 78.40 and 60.53 % compared to the P-ORC and ORC, respectively.

Tables 8, 9 and 10 show the power balance for each system analysed, where it is clear that the main consumer is the booster pump, while the seawater pump obtains very similar power consumption values. Regarding power generation, the turbine of the closed cycle in the P-ORC and ORC systems accounts for 49.94 and 82.99 % of the FSRU demand, respectively, while in the ORC-OC system it represents 78.09 %. However, in the latter system, the power of the OC turbine is equivalent to 14.62 % of the electrical power demand and, therefore, the total power produced by the turbines in the ORC-OC system satisfies 92.71 % of the demand.

Tables 11, 12 and 13 provide the exergy destroyed and exergy efficiency for each component of the P-ORC, ORC and ORC-OC systems, respectively. Among the evaluated systems, the component with the highest irreversibilities, i.e., exergy destroyed, is the condenser of the closed power cycle. This component represents 45.93, 32.72 and 26.31 % of the exergy destruction in the P-ORC, ORC and ORC-OC systems, respectively. Regarding the closed cycle exergy efficiency of the systems, the efficiency in the systems with zeotropic mixtures is more than double if compared to the value obtained for the P-ORC system (pure propane).

Table 7 Main results obtained from the energy, exergy and environmental analyses of the regasification systems

Cycle	Regasification system		
	P-ORC	**ORC**	**ORC-OC**
Wärtsilä 12V50DF load (%)	47.09	0.00	0.00
Wärtsilä 6L50DF load (%)	0.00	33.28	14.73
Electric power demand (kW)	10 184.49	10 596.70	10 953.06
Specific energy consumption (kJ/kg)	128.43	51.96	29.57
Exergy supplied (kW)	136 184.41	123 863.13	120 217.13
Exergy destruction (kW)	65 369.97	53 045.67	49 398.13
FSRU exergy efficiency (%)	52.00	57.17	58.91
EERI (g CO_2/MJ)	9.35	3.79	2.17
CFRI (g CO_2e/MJ)	11.79	4.65	2.55

Table 8 Electric power by equipment of the P-ORC system

Equipment	**Power (kW)**	$\eta_{el,m}$ **(%)**	**Electric power (kW)**	**Electric power weight (%)**
FSRU auxiliary services	-	-	2050.90	20.14
LD	213.65	80.00	267.06	2.62
P-1	257.66	90.00	286.29	2.81
P-2	3465.73	90.00	3850.81	37.81
P-3	144.15	90.00	160.17	1.57
P-4	3212.34	90.00	3569.26	35.05
T-1	5353.32	95.00	5085.65	49.94

Table 9 Electric power by equipment of the ORC system

Equipment	**Power (kW)**	$\eta_{el,m}$ **(%)**	**Electric power (kW)**	**Electric power weight (%)**
FSRU auxiliary services	-	-	2050.90	19.35
LD	213.91	80.00	267.39	2.52
P-1	257.25	90.00	285.84	2.70
P-2	3470.54	90.00	3856.16	36.39
P-3	379.70	90.00	421.89	3.98
P-4	3343.08	90.00	3714.53	35.05
T-1	9257.23	95.00	8794.36	82.99

Table 10 Electric power by equipment of the ORC-OC system

Equipment	Power (kW)	$\eta_{el,m}$ (%)	Electric power (kW)	Electric power weight (%)
FSRU auxiliary services	-	-	2050.90	18.72
LD	213.98	80.00	267.48	2.44
P-1	257.14	90.00	285.71	2.61
P-2	3774.67	90.00	4194.08	38.29
P-3	354.97	90.00	394.41	3.60
P-4	3384.44	90.00	3760.49	34.33
T-1	1686.11	95.00	1601.80	14.62
T-2	9003.57	95.00	8553.39	78.09

Table 11 Exergy results by equipment of the P-ORC system

Equipment	Fuel exergy (kW)	Product exergy (kW)	Irreversibility (kW)	Exergy efficiency (%)
CD-1	43 389.08	13 366.32	30 022.76	30.81
LD	213.65	103.62	110.03	48.50
MX	45.81	24.07	21.74	52.55
ORC (1)	43 389.08	5213.12	37 285.64	12.01
P-1	257.66	59.02	198.64	22.91
P-2	3465.73	870.28	2595.44	25.11
P-3	144.15	99.42	44.73	68.97
P-4	3212.34	2547.85	664.48	79.31
R	644.78	368.43	276.35	57.14
T-1	6964.31	5353.32	1610.99	76.87
TH	2464.48	194.73	2269.74	7.90
V-1	213.29	0.00	213.29	-
V-2	6.08	0.00	6.08	-
VP-1	6501.43	890.32	5611.12	13.69

Notes: (1) ORC equipment comprises all components through which the working fluid flows.

Table 12 Exergy results by equipment of the ORC system

Equipment	Fuel exergy (kW)	Product exergy (kW)	Irreversibility (kW)	Exergy efficiency (%)
CD-1	38 055.93	20 699.12	17 356.81	54.39
LD	213.91	103.75	110.16	48.50
MX	45.86	24.10	21.76	52.55
ORC (1)	38 055.93	8877.53	28 449.79	23.33
P-1	257.25	58.93	198.33	22.91
P-2	3470.54	880.76	2589.79	25.38
P-3	379.70	231.64	148.06	61.01
P-4	3343.08	2651.55	691.53	79.31
R	882.61	505.14	377.47	57.23
T-1	12 402.01	9257.23	3144.79	74.64
TH	7567.51	400.60	7166.91	5.29
V-1	212.95	0.00	212.95	-
V-2	8.36	0.00	8.36	-
VP-1	8528.74	728.61	7800.13	8.54

Notes: (1) ORC equipment comprises all components through which the working fluid flows.

Table 13 Exergy results by equipment of the ORC-OC system

Equipment	Fuel exergy (kW)	Product exergy (kW)	Irreversibility (kW)	Exergy efficiency (%)
CD-1	7895.69	5728.77	2166.92	72.56
CD-2	33 308.63	20 310.57	12 998.06	60.98
LD	213.98	103.79	110.20	48.50
MX	45.88	24.11	21.77	52.55
ORC (1)	33 308.63	8648.60	23 930.82	25.97
P-1	257.14	58.90	198.24	22.91
P-2	3774.67	984.01	2790.66	26.07
P-3	354.97	217.57	137.40	61.29
P-4	3384.44	2684.36	700.08	79.31
R	1500.12	1051.49	448.62	70.09
T-1	2548.19	1686.11	862.09	66.17
T-2	12 035.30	9003.57	3031.73	74.81
TH	7591.27	413.97	7177.30	5.45
V-1	212.86	0.00	212.86	-
V-2	9.02	0.00	9.02	-
VP-1	8492.83	729.21	7763.62	8.59

Notes: (1) ORC equipment comprises all components through which the working fluid flows.

4.3 Economics

Tables 14, 15 and 16 show the economic results obtained for the P-ORC, ORC and ORC-OC, respectively, which include the breakdown cost of the equipment and the total project cost obtained from APEA. The construction material and the type of heat exchangers have a significant influence on the total project cost of the systems. In general, SS316L steel is used as the construction material for the heat exchangers, however, in those where seawater flows, titanium is selected to avoid corrosion problems. Regarding the type of heat exchangers, all are of the shell and tube type except for the ORC vaporisers, which are plate heat exchangers. The choice of the latter instead of conventional shell and tube heat exchangers allows cost savings to be achieved. Among the systems evaluated, the P-ORC has the lowest total project cost and therefore the lowest capital investment cost rate. However, in the economic analysis, the effect of the LNG price on the total cost rate for each system must be considered as shown in Fig. 7. The P-ORC system is more cost effective than the other systems when the LNG price is below 7.116 USD/MMBtu (intersection point between the P-ORC and ORC lines). If the LNG price is between 7.116 and 11.298 USD/MMBtu (intersection point between the ORC and ORC-OC lines), the ORC system has the lowest total cost rate. For a higher fuel price, the most economical system is the ORC-OC. However, if the latter is compared to the P-ORC, the ORC-OC system has the lowest cost rate if the LNG price is higher than 8.065 USD/MMBtu.

Table 14 Economic results of the P-ORC system obtained from the APEA

Module	Equipment	n. º	Type / Material	Equip. cost (USD)	Installed cost (USD)	Total capital cost (USD)
Propane	Booster pump	2	CP / SS304	2 773 800	3 494 400	57 216 800
	Vaporizer	1	S&T / SS316L	69 200	346 200	
	Trim heater	1	S&T / Titanium	666 700	2 572 000	
	Propane pump	1	CP / SS304	350 600	748 300	
	Propane evaporator	3	PHE / Titanium	3 218 400	3 435 400	
P-ORC	P-2	4	CP / SS304	5 636 800	7 078 500	
	P-3	2	CP / SS304	865 800	2 342 500	
	CD-1	2	S&T / SS316L	1 390 600	5 311 400	
	T-1	2	-	1 024 800	3 213 900	
	VP-1	6	PHE / Titanium	37 500	225 100	
	TH	2	S&T / Titanium	1 293 800	5 112 300	

Notes: Centrifugal pump (CP), shell and tube heat exchanger (S&T) and plate heat exchanger (PHE).

Table 15 Economic results of the ORC system obtained from the APEA

Module	**Equipment**	**n. º**	**Type / Material**	**Equip. cost (USD)**	**Installed cost (USD)**	**Total capital cost (USD)**
Propane	Booster pump	2	CP / SS304	2 773 800	3 494 400	67 008 400
	Vaporizer	1	S&T / SS316L	350 600	748 300	
	Trim heater	1	S&T / Titanium	666 700	2 572 000	
	Propane pump	1	CP / SS304	37 500	225 100	
	Propane evaporator	3	PHE / Titanium	865 800	2 342 500	
ORC	P-2	4	CP / SS304	5 636 800	7 078 500	
	P-3	2	CP / SS304	316 000	549 700	
	CD-1	2	S&T / SS316L	3 871 200	9 348 500	
	T-1	2	-	4 476 400	4 753 300	
	VP-1	4	PHE / Titanium	876 800	2 419 500	
	TH	2	S&T / Titanium	1 922 600	6 929 000	

Notes: Centrifugal pump (CP), shell and tube heat exchanger (S&T) and plate heat exchanger (PHE).

Table 16 Economic results of the ORC-OC system obtained from the APEA

Module	Equipment	n. º	Type / Material	Equip. cost (USD)	Installed cost (USD)	Total capital cost (USD)
Propane	Booster pump	2	CP / SS304	2 773 800	3 494 400	71 544 200
	Vaporizer	1	S&T / SS316L	350 600	748 300	
	Trim heater	1	S&T / Titanium	666 700	2 572 000	
	Propane pump	1	CP / SS304	37 500	225 100	
	Propane evaporator	3	PHE / Titanium	865 800	2 342 500	
ORC-OC	P-2	4	CP / SS304	5 752 400	7 368 800	
	P-3	2	CP / SS304	310 000	543 300	
	CD-1	2	S&T / SS316L	478 800	2 935 500	
	CD-2	2	S&T / SS316L	2595000	7606800	
	T-1	2	-	853 800	1 187 200	
	T-2	2	-	4404600	4678700	
	VP-1	4	PHE / Titanium	812 400	2 329 800	
	TH	2	S&T / Titanium	1 978 000	6 987 300	

Notes: Centrifugal pump (CP), shell and tube heat exchanger (S&T) and plate heat exchanger (PHE).

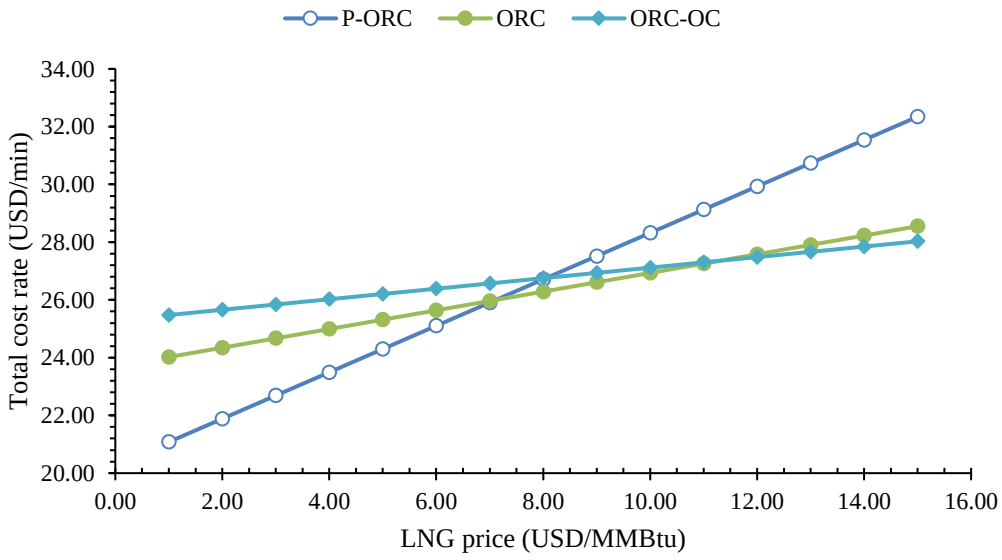

Fig. 7 Total cost rate comparison of the regasification systems analysed.

4.4 Comparison with regasification systems from previous works

The regasification systems analysed in this study are thermodynamically compared in Fig. 8 with the conventional systems installed onboard FSRUs: seawater system (SW-OL), open-loop propane system (P-OL) and closed-loop water-glycol system (WG-CL). In addition, a closed-loop regasification system with ORC and a CO_2 capture system (ORC-CC-CL) by chemical absorption evaluated in [40] are included in the comparison. The ORC-CC-CL system is able to fully satisfy the electrical power demand of the vessel and captures 90 % of the CO_2 emissions from the regasification boilers. Also included in the comparison are the 2ORC-OC and 3ORC-OC systems discussed in [26], which were designed to achieve the zero-carbon emissions target, i.e., these systems do not require fuel to be consumed in the DF engines. Fig. 8a shows that the specific consumption of any of the three ORC open-loop systems analysed is significantly lower than that of the most efficient conventional regasification system (SW-OL). Specifically, the P-ORC, ORC and ORC-OC systems reduce the specific energy consumption compared to SW-OL by 43.51, 77.14 and 86.99 %, respectively. Regarding the exergy analysis, Fig. 8b shows that the P-ORC, ORC and ORC-OC systems increase the efficiency by 3.99, 14.35 and 17.82 % with respect to the same open-loop regasification system. The systems analysed in this study do not achieve zero specific energy consumption, nor do they reach the exergy efficiencies of 2ORC-OC and 3ORC-OC systems, but the ORC-OC system offers thermodynamic results closer to zero-carbon emission systems than to conventional regasification systems.

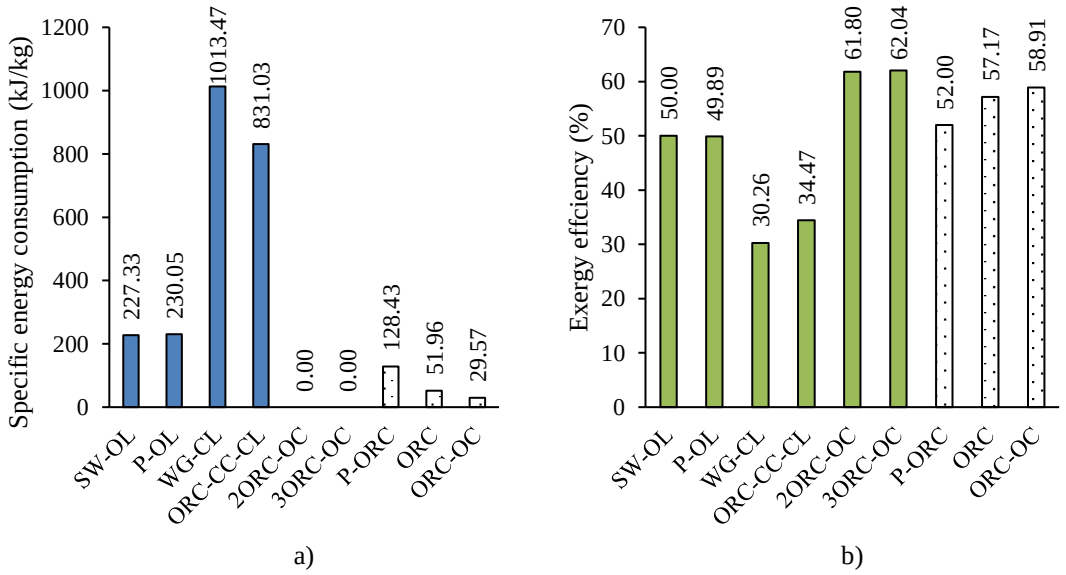

Fig. 8 Thermodynamic comparison of the regasification systems analysed in this study with those of the works [26,27,40]: a) specific energy consumption, b) FSRU exergy efficiency.

Fig. 9 provides the EERI and CFRI of the above systems to compare the CO_2 emissions during the regasification process on board the FSRU. In addition, two regasification systems previously evaluated in [9] have also been included: seawater system burning the BOG exceeding the consumption of the DF engines in the GCU (GCU-OL) and open-loop propane system with cold energy recovery by means of a simple ORC (ORC-OL) The comparison of the indicators is performed considering the same LNG composition in the regasification systems, which corresponds to the one presented in Table A. 3. The ORC-OL system is identical to the P-ORC, but gives slightly different results due to the different fluid packages implemented. The EERI values presented in Fig. 9a are a reflection of those obtained for the specific energy consumption in Fig. 8a. Regarding the CFRI, the three open-loop systems

analysed give in Fig. 9b a value of this indicator significantly lower than that obtained for conventional regasification systems. However, when comparing the CFRI of the three systems with the ORC-CC-CL, only the ORC-OC can achieve a lower level of CO_2e emissions, specifically, it reduces the CFRI by 22.46 %, being the closest system to zero-carbon emission systems (2ORC-OC and 3ORC-OC systems).

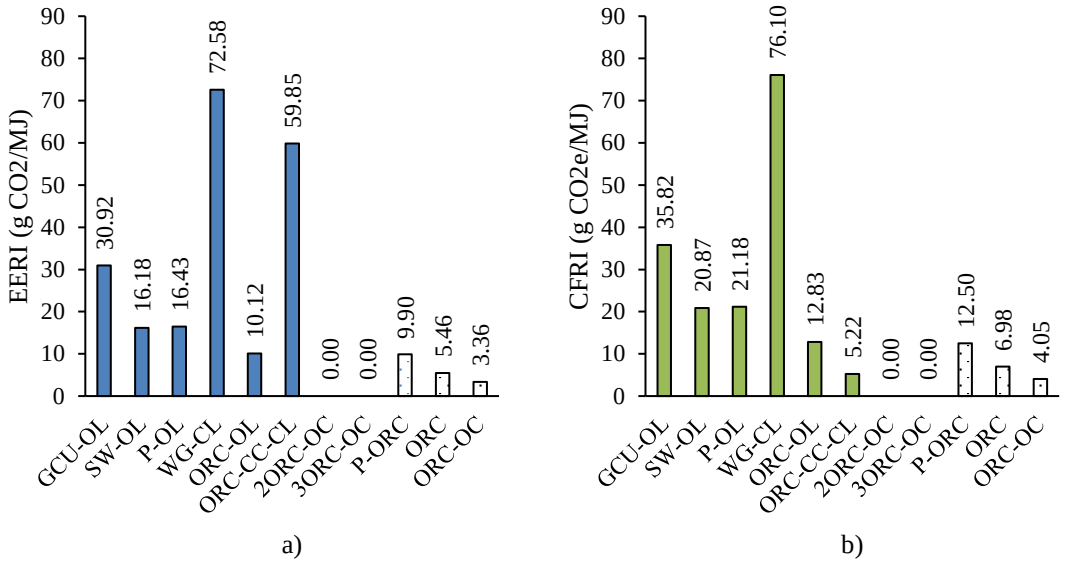

Fig. 9 Environmental comparison of the regasification systems analysed in this study with those of the works [9,26,40]: a) EERI, b) CFRI.

The three systems evaluated in this study are compared economically in Fig. 10 with the regasification systems that have been installed on FSRUs and the zero-carbon emission systems. The P-OL system is the most inexpensive of the conventional systems if the LNG price is above 1.320 USD/MMBtu. However, the P-ORC, ORC and ORC-OC systems have a lower total cost rate than the P-LA system if the fuel price is above 4.997, 5.905 and 6.508 USD/MMBtu (intersection points of the systems with respect to P-LA), respectively. The effect of the interest rate and the DO price at the intersection point of the three systems with the P-LA is shown in Figs. A 1 and A 2. Specifically, Fig. A 1 shows how the total cost rate varies at this point, while Fig. A 2 gives the corresponding LNG price. Both figures reveal that a low project interest rate and a high DO price leads to a lower total cost rate and LNG price at the intersection point and, consequently, widen the LNG price range where it is more economical to adopt the three evaluated systems with cold energy utilisation. However, the interest rate has a more significant impact than the DO price due to the low consumption of this hydrocarbon during the BOG combustion process in DF engines. If the regasification systems analysed in this study are compared with the most economical of the zero-carbon emission systems, i.e., the 2ORC-OC system, the intersection point occurs when the total cost rate is equal to 29.943 USD/min (36.188 USD/min in the case of the 3ORC-OC system). This is because the total cost rate of the latter systems is not influenced by the price of LNG and DO, as they do not have fuel consumption. Therefore, P-ORC, ORC and ORC-OC systems are more cost effective than zero-carbon emission systems when the LNG price is below 12.016, 19.299 and 25.496 USD/MMBtu, respectively.

In summary, the three cold energy utilisation systems analysed in this paper offer lower specific energy consumption and higher exergy efficiency than the conventional regasification systems adopted in FSRUs. This implies lower fuel consumption and a significant reduction of GHG emissions during the regasification process on board. The system with the best

thermodynamic and environmental performance is the ORC-OC. The level of GHG emissions for the ORC-OC is lower than that of the ORC-CC-CL, although the latter avoids fuel consumption in the DF engines and captures 90 % of the CO_2 emissions from the boiler. Regarding the economic analysis, any of the three systems is suitable to replace conventional regasification systems, as the minimum LNG prices for these systems to be cost-effective are lower than hydrocarbon prices both now and before the Covid-19 pandemic. When comparing the regasification systems analysed in this study with zero-carbon emissions systems, the thermodynamic and environmental results are worse, but not the economic performance. Therefore, they represent an intermediate alternative between conventional regasification systems and zero-carbon emission systems. Specifically, the ORC-OC system is the best positioned as it shows the widest LNG price range with the lowest total cost rate (6,508-25,496 USD/MMBtu).

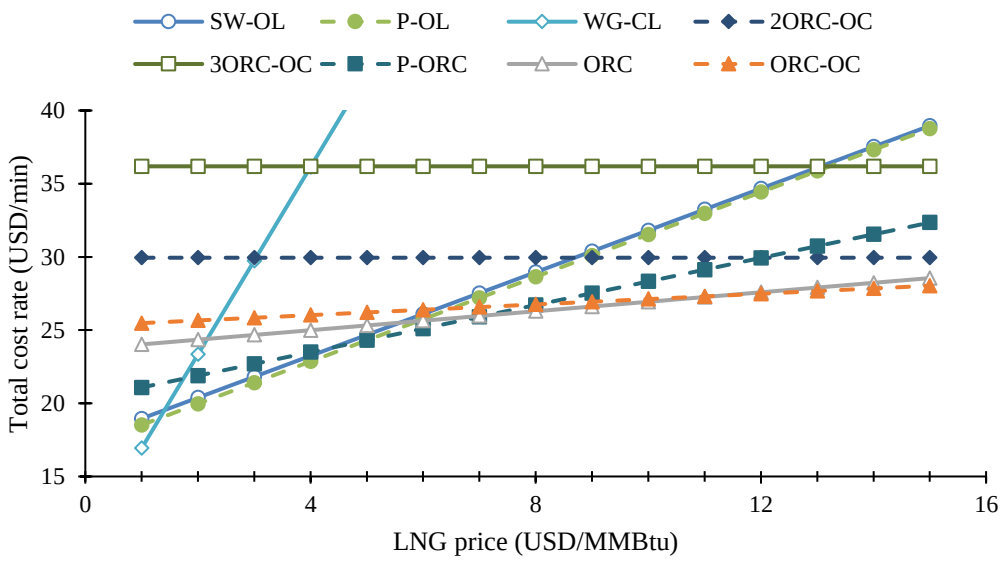

Fig. 10 Total cost rate comparison of the regasification systems analysed in this study with those of the works [26,27].

5. Conclusions

In this paper, an open-loop regasification system for FSRUs that combines a simple ORC with an OC (ORC-OC) to reduce GHG emissions during the regasification process from an energy, exergy, economic and environmental standpoint. The main conclusions of the study are as follows:

- The composition of the LNG to be regasified influences the electrical power produced by the system and, consequently, the power to be generated by the FSRU's power generation plant, i.e., the DF engines. This is particularly relevant when a zeotropic ethane/propane mixture is used as the ORC working fluid in order to minimise the power to be produced by the DF engines. Thus, the ORC-OC system with the working fluid optimal composition reduces the power to be generated in the DF engines up to 84.35 and 55.73 % with respect to the P-ORC (simple ORC with pure propane) and ORC (simple ORC with zeotropic mixture), respectively. These values decrease to 73.37 and 54.40 % if a real LNG composition with 89 % methane is used (Table A. 3).
- The energy analysis indicates that the ORC-OC system reduces the specific energy consumption of the FSRU by 76.97 and 59.54 % compared to the P-ORC and ORC,

respectively, offering a more efficient cold energy recovery system than those commonly considered in publications. In addition, the ORC-OC system has the highest exergy efficiency and the lowest CFRI. Regarding the latter parameter, the proposed system reduces CO_2e emissions by 78.40 and 60.53 % when compared to P-ORC and ORC systems. Regarding the economic analysis, the ORC-OC system is more economical than the other two systems if the LNG price is higher than 8.065 and 11.298 USD/MMBtu, respectively.

- The comparison of the systems considered in this study with the conventional regasification systems adopted in the FSRUs suggests that the ORC-OC system offers a more efficient and environmentally friendly regasification process. If the most efficient conventional regasification system, i.e., the seawater system (SW-OL), is taken as a reference, the ORC-OC reduces the specific energy consumption by 86.99 % and increases the energy efficiency by 17.82 %, obtaining a significant reduction in fuel consumption and, consequently, in GHG emissions. Compared to the most economical regasification system installed on board, the propane open loop (P-OL) system, the ORC-OC system has a lower total cost rate if the LNG price is higher than 6.508 USD/MMBtu. Considering both current and pre-Covid-19 LNG prices, the proposed system offers a more economical regasification system for a wide range of hydrocarbon prices.
- The regasification systems analysed in this paper are an intermediate alternative to the zero-carbon emissions regasification systems (2ORC-OC and 3ORC-OC systems). Although the systems evaluated do not achieve zero fuel consumption, they are more attractive from an economic point of view. Specifically, the ORC-OC system is the closest to the zero-carbon emission target and shows the widest LNG price range where it is economical, representing the best alternative for installation on a regasification vessel.

The utilisation of the LNG cold energy can improve energy efficiency and drastically reduce GHG emissions from the regasification process of FSRUs. Investment in regasification systems capable of exploiting cold energy becomes imperative if a more environmentally friendly regasification process is to be achieved.

REFERENCES

[1] International Energy Agency, 2022. Gas Market Report Q3 2022.

[2] International Energy Agency, 2022. A 10-Point Plan to Reduce the European Union' s Reliance on Russian Natural Gas.

[3] IGU, 2022. 2022 World LNG Report.

[4] Mokhatab, S., Mak, J. Y., Valappil, J. V., Wood, D. A., 2014. Handbook of Liquefied Natural Gas. *Elsevier*.

[5] Mauro, F., Braidotti, L., Trincas, G., 2019. Determination of an optimal fleet for a cng transportation scenario in the mediterranean sea. *Brodogradnja*, 70(3), 1-23. https://doi.org/10.21278/brod70301

[6] Songhurst, B., 2017. The Outlook for Floating Storage and Regasification Units (FSRUs). Oxford, United Kingdom. https://doi.org/10.26889/9781784670894

[7] IMO, 2011. MEPC.203(62) Amendments to MARPOL Annex VI on regulations for the prevention of air pollution from ships by inclusion of new regulations on energy efficiency for ships.

[8] IMO, 2021. MEPC.328(76) Amendments to the Annex of the Protocol of 1997 to amend the International Convention for the Prevention of Pollution from Ships, 1973, as modified by the Protocol of 1978 relating there to 2021 Revised MARPOL Annex VI.

[9] Naveiro, M., Romero Gómez, M., Arias Fernández, I., Baaliña Insua, Á., 2021. Energy efficiency and environmental measures for Floating Storage Regasification Units. *Journal of Natural Gas Science and Engineering*, 96, 104271. https://doi.org/10.1016/j.jngse.2021.104271

[10] Kanbur, B. B., Xiang, L., Dubey, S., Choo, F. H., Duan, F., 2017. Cold utilization systems of LNG: A review. *Renewable and Sustainable Energy Reviews*, 79, 1171-1188. https://doi.org/10.1016/j.rser.2017.05.161

[11] He, T., Chong, Z. R., Zheng, J., Ju, Y., Linga, P., 2019. LNG cold energy utilization: Prospects and challenges. *Energy*, 170, 557-568. https://doi.org/10.1016/j.energy.2018.12.170

[12] Naveiro, M., Romero Gómez, M., Arias Fernández, I., Romero Gómez, J., 2021. Exploitation of liquefied natural gas cold energy in floating storage regasification units. *Brodogradnja*, 72(4), 47-78. https://doi.org/10.21278/brod72404

[13] Mitsui O.S.K. Lines, 2020. MOL and DSME Obtain AIP for Design of FSRU "Cryo-Powered Regas" System - Development of New Technology to Reduce Environmental Impact -. https://www.mol.co.jp/en/pr/2020/20016.html. accessed 20th October 2022.

[14] Romero Gómez, M., Ferreiro Garcia, R., Romero Gómez, J., Carbia Carril, J., 2014. Review of thermal cycles exploiting the exergy of liquefied natural gas in the regasification process. *Renewable and Sustainable Energy Reviews*, 38, 781-795. https://doi.org/10.1016/j.rser.2014.07.029

[15] Mehrpooya, M., Sharifzadeh, M. M. M., Katooli, M. H., 2018. Thermodynamic analysis of integrated LNG regasification process configurations. *Progress in Energy and Combustion Science*, 69, 1-27. https://doi.org/10.1016/j.pecs.2018.06.001

[16] Pospíšil, J., Charvát, P., Arsenyeva, O., Klimeš, L., Špiláček, M., Klemeš, J. J., 2019. Energy demand of liquefaction and regasification of natural gas and the potential of LNG for operative thermal energy storage. *Renewable and Sustainable Energy Reviews*, 99, 1-15. https://doi.org/10.1016/j.rser.2018.09.027

[17] Modi, A., Haglind, F., 2017. A review of recent research on the use of zeotropic mixtures in power generation systems. *Energy Conversion and Management*, 138, 603-626. https://doi.org/10.1016/j.enconman.2017.02.032

[18] Xu, W., Zhao, R., Deng, S., Zhao, L., Mao, S. S., 2021. Is zeotropic working fluid a promising option for organic Rankine cycle: A quantitative evaluation based on literature data. *Renewable and Sustainable Energy Reviews*, 148, 111267. https://doi.org/10.1016/j.rser.2021.111267

[19] Yao, S., Liu, H., Tang, L., Ye, Y., Zhang, L., 2016. Thermodynamic analysis and optimization for cold energy utilization based on low temperature rankine cycle of LNG-FSRU regasification system. *International Journal of Simulation: Systems, Science and Technology*, 17(30), 35.1-35.9.

[20] Lee, S., Choi, B.C., 2016. Thermodynamic assessment of integrated heat recovery system combining exhaust-gas heat and cold energy for LNG regasification process in FSRU vessel. *Journal of Mechanical Science and Technology*, 30(3), 1389-1398. https://doi.org/10.1007/s12206-016-0246-y

[21] Yoon-Ho, L., 2019. Thermo-economic analysis of a novel regasification system with liquefied-natural-gas cold-energy. *International Journal of Refrigeration*, 101, 218-229. https://doi.org/10.1016/j.ijrefrig.2019.03.022

[22] Yao, S., Xu, L., Tang, L., 2019. New cold-level utilization scheme for cascade three-level Rankine cycle using the cold energy of liquefied natural gas. *Thermal Science*, 23(6B), 3865-3875. https://doi.org/10.2298/TSCI171012239Y

[23] Xu, L., Lin, G., 2021. Simulation and optimization of liquefied natural gas cold energy power generation system on floating storage and regasification unit. *Thermal Science*, 25(6B), 4707-4719. https://doi.org/10.2298/TSCI200404205X

[24] Yoon-Ho, L., 2019. LNG-FSRU cold energy recovery regasification using a zeotropic mixture of ethane and propane. *Energy*, 173, 857-869. https://doi.org/10.1016/j.energy.2019.02.111

[25] Mak, J. Y., 2005. Configurations and methods for power generation with integrated LNG regasification. WO 2006/019900 A1.

[26] Naveiro, M., Romero Gómez, M., Arias-Fernández, I., Baaliña Insua, Á., 2021. Thermodynamic and Economic Analyses of Zero-Emission Open Loop Offshore Regasification Systems Integrating ORC with Zeotropic Mixtures and LNG Open Power Cycle. *Energies*, 15(22), 8622. https://doi.org/10.3390/en15228622

[27] Naveiro, M., Romero Gómez, M., Baaliña Insua, Á., Folgueras, M. B., 2021. Energy, exergy and economic analysis of offshore regasification systems. *International Journal of Energy Research*, 45(15), 20835-20866. https://doi.org/10.1002/er.7141

[28] Ammar, N. R., 2019. Environmental and cost-effectiveness comparison of dual fuel propulsion options for emissions reduction onboard lng carriers. *Brodogradnja* ,70(3), 61-77. https://doi.org/10.21278/brod70304

[29] Romero Gómez, J., Romero Gómez, M., Lopez Bernal, J., Baaliña Insua, A., 2015. Analysis and efficiency enhancement of a boil-off gas reliquefaction system with cascade cycle on board LNG carriers. *Energy Conversion and Management*, 94, 261-274. https://doi.org/10.1016/j.enconman.2015.01.074

[30] Frangopoulos, C.A., 2009. Exergy, Energy System Analysis and Optimization Volume - I: Exergy and Thermodynamic Analysis. *EOLSS Publications*, Oxford, United Kingdom.

[31] Szargut, J., 2005. Exergy method: technical and ecological applications. *WIT Press*.

[32] Bejan, A., Tsatsaronis, G., Moran, M., 1996. Thermal Design and Optimization. *John Wiley & Sons, Ltd*.

[33] Aspen Technology, 2019. Suite AspenONE.

[34] Querol, E., Gonzalez-Regueral, B., Perez-Benedito, J. L., 2013. Practical Approach to Exergy and Thermoeconomic Analyses of Industrial Processes. *Springer London*. https://doi.org/10.1007/978-1-4471-4622-3

[35] Chemical Engineering, 2020. CEPCI Archives 2020. https://www.chemengonline.com/tag/cepci/. accessed 5th September 2020.

[36] IMO, 2018. MEPC.308(73) 2018 Guidelines on the method of calculation of the attained Energy Efficiency Design Index (EEDI) for new ships.

[37] Huang, J., Mendoza, B., Daniel, J. S., Nielsen, C. J., Rotstayn, L., Wild, O., 2013. Anthropogenic and natural radiative forcing. In Climate Change 2013 – The Physical Science Basis: Working Group I Contribution to the Fifth Assessment Report of the Intergovernmental Panel on Climate Change. *Cambridge University Press*.

[38] Pavlenko, N., Comer, B., Zhou, Y., Clark, N., Rutherford, D., 2020. The climate implications of using LNG as a marine fuel.

[39] IMO, 2020. MEPC 75/7/15 Reduction of GHG emissions from ships: Fourth IMO GHG Study 2020 - Final Report.

[40] Naveiro, M., Romero Gómez, M., Arias-Fernández, I., Baaliña Insua, Á., 2022. Thermodynamic and environmental analyses of a novel closed loop regasification system integrating ORC and CO2 capture in floating storage regasification units. *Energy Conversion and Management*, 257, 15410. https://doi.org/10.1016/j.enconman.2022.115410

APPENDIX A

Table A. 1 General specifications of the model FSRU [40]

Item	Value
Type of LNG storage tanks	MARK III, maximum vapour pressure of 0.7 bar(g) and boil off rate (BOR) of 0.15 %
Cargo capacity	170 000 m^3
Type of LD compressor	2 stage centrifugal compressor with pre-cooling
Maximum / baseload regasification capacity	750 mmscfd / 500 mmscfd
Propulsion system	Dual fuel diesel electric (DFDE)
Engines	3 x Wärtsilä 12V50DF (11.4 MW) 1 x Wärtsilä 6L50DF (5.7 MW)

Table A. 2 Specific energy consumption of 50DF engines [27]

Load (%)	Specific energy consumption (kJ/kW h)	
	Natural gas	Pilot DO
25	11 922.7	234.4
50	9286.7	77.2
75	8258.4	30.1
100	7665.4	19.2

Table A. 3 Composition of NG measured on board an FSRU [12]

Component	Mole fraction
Methane	0.89018
Nitrogen	0.00007
Carbon dioxide	0.00000
Ethane	0.07974
Propane	0.02291
i-Butane	0.00322
n-Butane	0.00371
i-Pentane	0.00014
n-Pentane	0.00002
n-Hexane	0.00001

Table A. 4 Parameters assumed in the study of regasification systems

Parameter	Value
LNG tank pressure	1.16325 bar
BOG temperature from tank	-100 ºC
Regasified NG mass flow rate	111.19 kg/s
Regasified NG pressure	85 bar
Regasified NG temperature	10 ºC
Pumps and turbines isentropic efficiency	80 %
Pumps and turbines electromechanical efficiency	90 %
Feed pump discharge pressure	9 bar
LD isentropic efficiency	55 %
LD electromechanical efficiency	80 %
BOG temperature after the mixer	-120 ºC
LD discharge pressure	6 bar
Recondenser pressure	5.5 bar
Minimum temperature difference in heat exchangers	5 ºC
Pressure drop in heat exchangers	0.5 bar
Condensation pressure	1.5 bar
LNG pressure drop through CD-1	21 bar
NG pressure drop through heat exchangers	2 bar
Sea water inlet temperature	15 ºC
Sea water outlet temperature	10 ºC
Sea water inlet pressure	1.01325 bar
Sea water pump discharge pressure	7.5 bar

Table A. 5 Thermodynamic data of the P-ORC system

State	Quality (-)	T (ºC)	p (bar)	h (kJ/kg)	s (kJ/kg K)	e^{ph} (kJ/kg)	$\dot{m}$ (kg/s)
1	0.0000	-159.89	1.16325	-5573.11	4.8145	21.28	110.73
2	0.0000	-159.49	9.00	-5570.79	4.8205	334.78	110.73
3	0.0000	-159.37	5.50	-5570.79	4.8269	259.86	110.73
4	0.0000	-158.34	5.50	-5567.17	4.8586	259.86	111.19
5	0.0000	-152.92	110.00	-5536.00	4.9369	691.43	111.19
6	0.0000	-159.89	1.16325	-5573.11	4.8145	21.28	0.05
7	0.0000	-159.89	1.16325	-5573.11	4.8145	21.28	0.05
8	0.0000	-159.89	1.16325	-5573.11	4.8145	21.28	0.00
9	1.0000	-120.00	1.16325	-4979.77	9.9474	21.28	0.00
10	1.0000	-100.00	1.16325	-4938.05	10.2034	21.28	0.70
11	1.0000	-100.00	1.16325	-4938.05	10.2034	21.28	0.70
12	1.0000	-120.00	1.16325	-4979.77	9.9474	21.28	0.74
13	0.0000	-120.00	1.16325	-5418.49	5.9764	21.28	0.00
14	1.0000	-120.00	1.16325	-4979.77	9.9474	21.28	0.74
15	1.0000	17.43	6.00	-4692.66	10.4433	273.13	0.74
16	1.0000	17.43	6.00	-4692.66	10.4433	273.13	0.46
17	1.0000	17.17	5.50	-4692.66	10.4878	259.86	0.46
18	1.0000	17.43	6.00	-4692.66	10.4433	273.13	0.29
19	1.0000	35.00	5.90	-4652.48	10.5861	270.57	0.29
20	1.0000	35.00	5.90	-4652.48	10.5861	270.57	0.29
21	1.0000	35.00	5.90	-4652.48	10.5861	270.57	0.00
22	1.0000	-30.30	87.00	-4946.94	8.2214	661.25	111.19
23	1.0000	10.00	85.00	-4807.86	8.7622	658.21	111.19
24	0.0000	-32.84	1.50	-2867.36	1.5179	21.60	154.09
25	0.0000	-32.56	5.77	-2866.43	1.5189	93.23	154.09
26	1.0000	3.55	5.27	-2407.57	3.1994	88.62	154.09
27	1.0000	-25.09	2.00	-2442.31	3.2345	37.30	154.09
28	0.0000	15.00	1.01325	15 907.22	5.0369	0.00	3958.14
29	0.0000	15.05	7.50	-15 906.41	5.0375	0.65	3958.14
30	0.0000	15.05	7.50	-15 906.41	5.0375	0.65	710.36
31	0.0000	10.00	1.01325	-15 928.18	4.9635	0.00	710.36
32	0.0000	15.05	7.50	-15 906.41	5.0375	0.65	3247.77
33	0.0000	10.00	1.01325	-15 928.18	4.9635	0.00	3247.77
34	0.0000	36.00	2.50	-15 819.26	5.3311	0.15	8.33
35	0.0000	35.67	2.35	-15 820.63	5.3267	0.13	8.33

Table A. 6 Thermodynamic data of the ORC system

State	Quality (-)	T (ºC)	p (bar)	h (kJ/kg)	s (kJ/kg K)	e^{ph} (kJ/kg)	$\dot{m}$ (kg/s)
1	0.0000	-159.89	1.16325	-5573.11	4.8145	1071.14	110.56
2	0.0000	-159.49	9.00	-5570.79	4.8205	1071.68	110.56
3	0.0000	-159.37	5.50	-5570.79	4.8269	1069.75	110.56
4	0.0000	-157.95	5.50	-5565.81	4.8704	1061.77	111.19
5	0.0000	-152.51	110.00	-5534.60	4.9485	1069.69	111.19
6	0.0000	-159.89	1.16325	-5573.11	4.8145	1071.14	0.05
7	0.0000	-159.89	1.16325	-5573.11	4.8145	1071.14	0.05
8	0.0000	-159.89	1.16325	-5573.11	4.8145	1071.14	0.00
9	1.0000	-120.00	1.16325	-4979.77	9.9474	134.10	0.00
10	1.0000	-100.00	1.16325	-4938.05	10.2034	99.48	0.70
11	1.0000	-100.00	1.16325	-4938.05	10.2034	99.48	0.70
12	1.0000	-120.00	1.16325	-4979.77	9.9474	134.10	0.75
13	0.0000	-120.00	1.16325	-5418.49	5.9764	879.32	0.00
14	1.0000	-120.00	1.16325	-4979.77	9.9474	134.10	0.75
15	1.0000	17.43	6.00	-4692.66	10.4433	273.35	0.75
16	1.0000	17.43	6.00	-4692.66	10.4433	273.35	0.63
17	1.0000	17.17	5.50	-4692.66	10.4878	260.09	0.63
18	1.0000	17.43	6.00	-4692.66	10.4433	273.35	0.11
19	1.0000	35.00	5.90	-4652.48	10.5861	270.95	0.11
20	1.0000	35.00	5.90	-4652.48	10.5861	270.95	0.11
21	1.0000	35.00	5.90	-4652.48	10.5861	270.95	0.00
22	1.0000	-58.19	87.00	-5094.00	7.5742	727.43	111.19
23	1.0000	10.00	85.00	-4807.86	8.7622	659.37	111.19
24	0.0000	-75.78	1.50	-3298.17	2.7132	276.59	105.07
25	0.0000	-74.84	17.59	-3294.56	2.7179	278.79	105.07
26	1.0000	10.05	17.09	-2743.80	4.8374	197.62	105.07
27	0.9424	-53.19	2.00	-2831.90	4.9378	79.58	105.07
28	0.0000	15.00	1.01325	15 907.22	5.0369	0.72	4119.23
29	0.0000	15.05	7.50	-15 906.41	5.0375	1.36	4119.23
30	0.0000	15.05	7.50	-15 906.41	5.0375	1.36	1461.35
31	0.0000	10.00	1.01325	-15 928.18	4.9635	1.64	1461.35
32	0.0000	15.05	7.50	-15 906.41	5.0375	1.36	2657.88
33	0.0000	10.00	1.01325	-15 928.18	4.9635	1.64	2657.88
34	0.0000	36.00	2.50	-15 819.26	5.3311	0.98	8.33
35	0.0000	35.87	2.35	-15 819.81	5.3293	0.94	8.33

Table A. 7 Thermodynamic data of the ORC-OC system

State	Quality (-)	T (ºC)	p (bar)	h (kJ/kg)	s (kJ/kg K)	e^{ph} (kJ/kg)	$\dot{m}$ (kg/s)
1	0.0000	-159.89	1.16325	-5573.11	4.8145	1071.14	110.51
2	0.0000	-159.49	9.00	-5570.79	4.8205	1071.68	110.51
3	0.0000	-159.37	5.50	-5570.79	4.8269	1069.75	110.51
4	0.0000	-156.94	5.50	-5562.26	4.9010	1056.17	120.49
5	0.0000	-151.43	110.00	-5530.94	4.9787	1064.34	120.49
6	0.0000	-159.89	1.16325	-5573.11	4.8145	1071.14	0.05
7	0.0000	-159.89	1.16325	-5573.11	4.8145	1071.14	0.05
8	0.0000	-159.89	1.16325	-5573.11	4.8145	1071.14	0.00
9	1.0000	-120.00	1.16325	-4979.77	9.9474	134.10	0.00
10	1.0000	-100.00	1.16325	-4938.05	10.2034	99.48	0.70
11	1.0000	-100.00	1.16325	-4938.05	10.2034	99.48	0.70
12	1.0000	-120.00	1.16325	-4979.77	9.9474	134.11	0.75
13	0.0000	-120.00	1.16325	-5418.49	5.9764	879.33	0.00
14	1.0000	-120.00	1.16325	-4979.77	9.9474	134.10	0.75
15	1.0000	17.43	6.00	-4692.66	10.4433	273.35	0.75
16	1.0000	17.43	6.00	-4692.66	10.4433	273.35	0.68
17	1.0000	17.17	5.50	-4692.66	10.4878	260.10	0.68
18	1.0000	17.43	6.00	-4692.66	10.4433	273.35	0.06
19	1.0000	35.00	5.90	-4652.48	10.5861	270.95	0.06
20	1.0000	35.00	5.90	-4652.48	10.5861	270.95	0.06
21	1.0000	35.00	5.90	-4652.48	10.5861	270.95	0.00
22	1.0000	10.00	85.00	-4807.86	8.7622	659.37	9.30
23	1.0000	-117.34	6.00	-4989.16	9.0731	385.37	9.30
24	0.0000	-146.42	5.50	-5524.60	5.2112	1001.36	9.30
25	0.0000	-138.81	89.00	-5489.61	5.3371	998.81	120.49
26	1.0000	-56.28	87.00	-5080.73	7.6357	722.37	120.49
27	1.0000	10.00	85.00	-4807.86	8.7622	659.37	120.49
28	1.0000	10.00	85.00	-4807.86	8.7622	659.37	111.19
29	0.0000	-75.00	1.50	-3278.93	2.6523	269.99	105.14
30	0.0000	-74.12	16.59	-3275.56	2.6567	272.06	105.14
31	1.0000	10.05	16.09	-2724.73	4.7751	191.29	105.14
32	0.9466	-51.28	2.00	-2810.37	4.8718	76.82	105.14
33	0.0000	15.00	1.01325	15 907.22	5.0369	0.72	4170.20
34	0.0000	15.05	7.50	-15 906.41	5.0375	1.36	4170.20
35	0.0000	15.05	7.50	-15 906.41	5.0375	1.36	1510.11
36	0.0000	10.00	1.01325	-15 928.18	4.9635	1.64	1510.11
37	0.0000	15.05	7.50	-15 906.41	5.0375	1.36	2660.08
38	0.0000	10.00	1.01325	-15 928.18	4.9635	1.64	2660.08
39	0.0000	36.00	2.50	-15 819.26	5.3311	0.98	8.33
40	0.0000	35.93	2.35	-15 819.57	5.3301	0.95	8.33

Table A. 8 Molar compositions and chemical exergies of the P-ORC system

State	Composition (mol %)				e^{ch}
	Methane	Ethane	Propane	Water	(kJ/kg)
1-23	100.00	0.00	0.00	0.00	51 480.00
24-27	0.00	0.00	100.00	0.00	-
28-35	0.00	0.00	0.00	100.00	-

Table A. 9 Molar compositions and chemical exergies of the ORC system

State	Composition (mol %)				e^{ch}
	Methane	Ethane	Propane	Water	(kJ/kg)
1-23	100.00	0.00	0.00	0.00	51 480.00
24-27	0.00	76.00	24.00	0.00	-
28-35	0.00	0.00	0.00	100.00	-

Table A. 10 Molar compositions and chemical exergies of the ORC-OC system

State	Composition (mol %)				e^{ch}
	Methane	Ethane	Propane	Water	(kJ/kg)
1-28	100.00	0.00	0.00	0.00	51 480.00
29-32	0.00	73.00	27.00	0.00	-
33-40	0.00	0.00	0.00	100.00	-

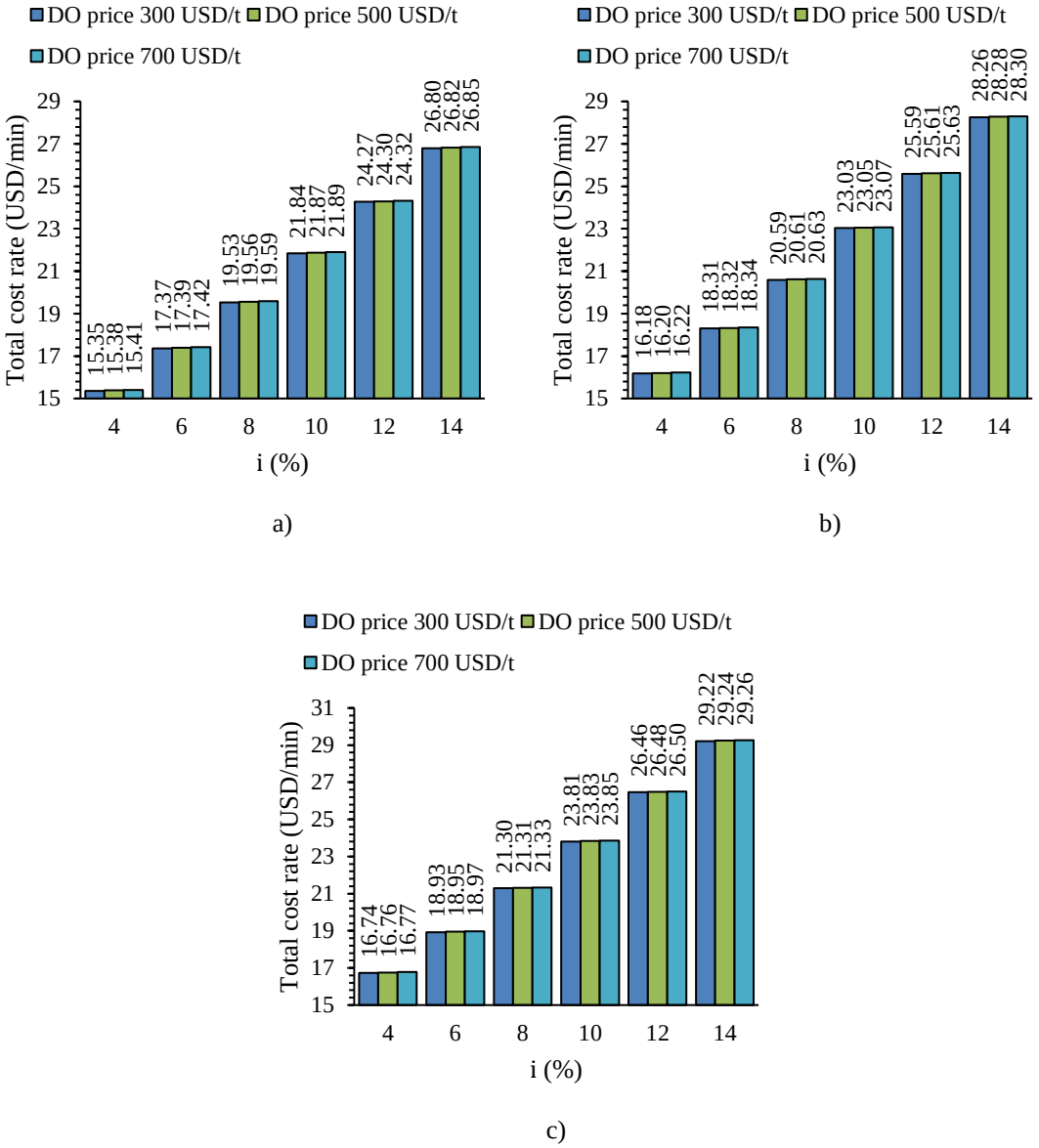

Fig. A 1 Variation of the total cost rate at the intersection point with the DO price and the project interest rate: a) P-ORC, b) ORC, c) ORC-OC.

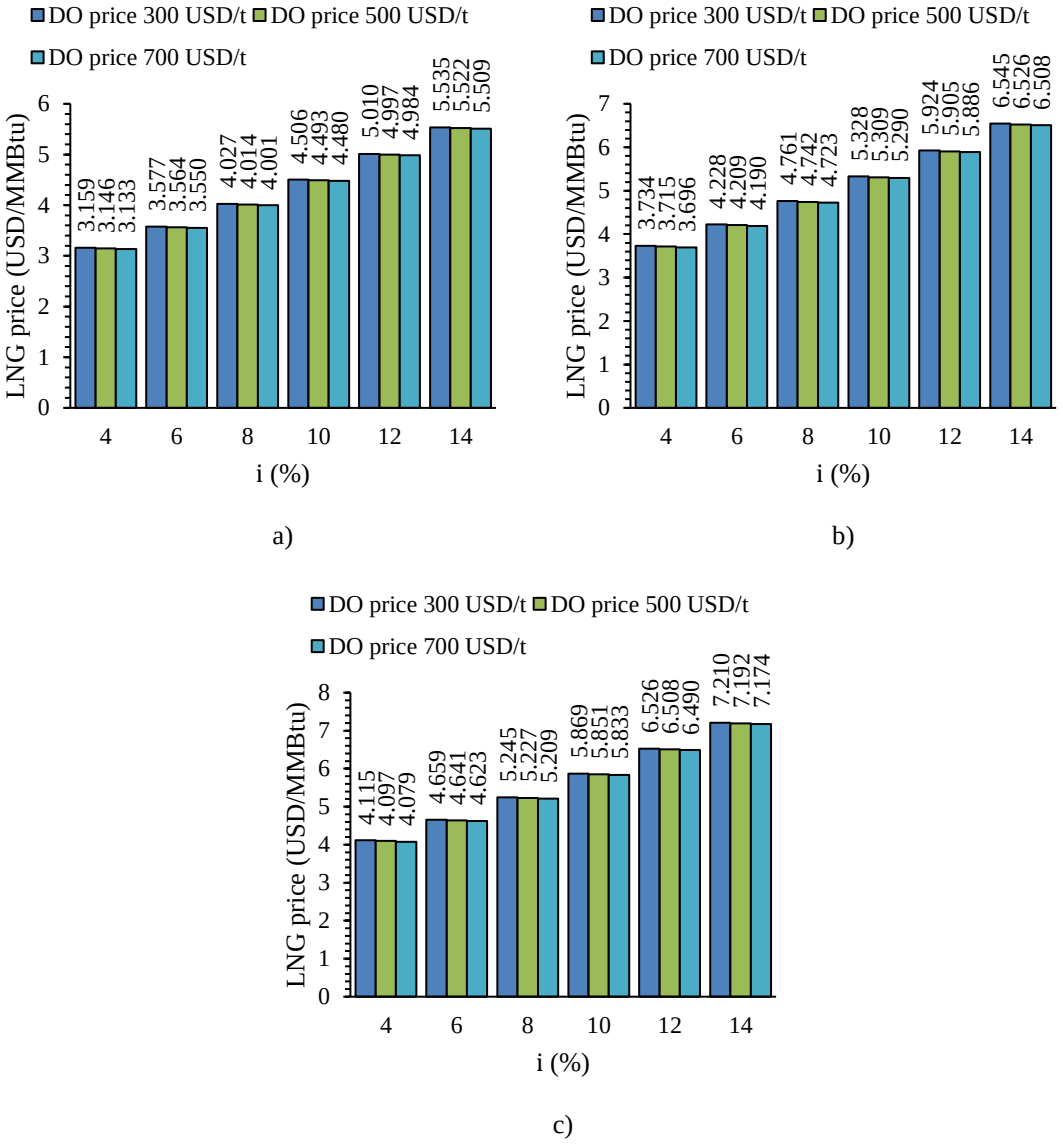

Fig. A 2 Variation of the LNG price at the intersection point with the DO price and the project interest rate: a) P-ORC, b) ORC, c) ORC-OC.

Submitted: 27.11.2022.

Accepted: 08.03.2023.

Manuel Naveiro, manuel.naveiro@udc.es
Energy Engineering Research Group, University Institute of Maritime Studies, ETSNM, University of A Coruña, Paseo de Ronda 51, A Coruña 15011, Spain
Manuel Romero Gómez, m.romero.gomez@udc.es
Energy Engineering Research Group, University Institute of Maritime Studies, Nautical Sciences and Marine Engineering Department, ETSNM, University of A Coruña, Paseo de Ronda 51, A Coruña 15011, Spain
Ignacio Arias-Fernández, ignacio.arias@udc.es
Energy Engineering Research Group, University Institute of Maritime Studies, Nautical Sciences and Marine Engineering Department, ETSNM, University of A Coruña, Paseo de Ronda 51, A Coruña 15011, Spain
Álvaro Baaliña Insua, alvaro.baalina@udc.es
Energy Engineering Research Group, University Institute of Maritime Studies, Nautical Sciences and Marine Engineering Department, ETSNM, University of A Coruña, Paseo de Ronda 51, A Coruña 15011, Spain